Mach 5, 2022, V1

Grand Unified Theory of Mind and Brain

Part II
Neural Holographic Tomography (NHT) and Holographic Ring Attractor Lattice (HAL)

Katsushi Arisaka

University of California, Los Angeles
Department of Physics and Astronomy,
Department of Electrical and Computer Engineering
475 Portola Plaza, Los Angeles, CA 90095, USA
Contact: arisaka@physics.ucla.edu

Abstract

For animals to navigate a given space, it is essential to perceive and memorize the external allocentric frame with landmarks. In the previous **Part I** (Arisaka 2022), by applying causality and locality at every single synapse, we proposed a new concept of **MePMoS**. This model allowed constructing the complete space-time dynamic connectomes of *C. elegans* and human brains.

This **Part II** proposes a generic principle of space-to-time conversion for perceiving 3D space and 3D shape in a frequency-time domain, named **Neural Holographic Tomography (NHT)**. In this general model, three strings of one-dimensional neurons can encode 3D space, utilizing the spike timings expressed by the phases of brainwaves. Therefore, dynamic shifting of phases can accomplish natural translation from an ever-changing egocentric frame acquired from sensory input to the perception of a stable allocentric frame, resulting in the steady perception of allocentric 3D space.

We further propose a universal unit of memory, an engram named **HAL (Holographic Ring Attractor Lattice)**. Facilitated by Hebbian plasticity, the phases of brainwaves, representing 3D space and shape, are registered by the 2D matrix of synaptic networks to form long-term static memories. This two-step conversion of sensory stimulation, first to a brainwave phase by **NHT** and second to synaptic memory by **HAL**, provides a general principle for perception and memory of allocentric 3D space and semantic 3D shape.

Table of Contents

Abbreviations

Abbreviation	Definition
AIP	Anterior Intraparietal area
AIT	Anterior Inferior Temporal cortex
CA	Cornu Ammonis
CIP	Caudal Intraparietal area
CNS	Central Nurvous System
CPG	Central Pattern Generator
CRT	Choice Reaction Time
DFT	Descrete Fourier Transformation
DG	Dentate Gyrus
ECoG	Electrocorticography
EEG	Electroencephalography
GUT	**Grand Unified Theory**
HAL	**Holographic Ring Attractor Lattice**
HC	Hippocampus
HCN	Hippocampal Network
iEEG	Invasive Electroencephalography
LEC	Lateral Entorhinal Cortex
LFP	Local Field Potential
LGN	Lateral Geniculate Nucleus
LIP	Lateral Intraparietal cortex
LTD	Long-term Depression
LTP	Long-term Potentiation
MEC	Medial Entorhinal Cortex
MEG	Magnetoencephalography
MePMoS	**Memory-Prediction-Motion-Sensing**
MIP	Medial Intraparietal cortex
MST	Medial Superior Temporal area
MT	Middle-Temporal Area
NHT	**Neural Holographic Tomography**
PFC	Prefrontal Cortex
PIT	Posterior Inferior Temporal cortex
PN	Pulvinar Nuclei
RF	Receptive Field
RSC	Retrosplenial Cortex
RT	Reaction Time
SAC	Somatosensory Association Cortex (Brodmann Areas 5 and 7)
SC	Superior Colliculus
SRT	Simple Reation Time
STDP	Spike Timing-Dependent Plasticity
SWR	Sharp Wave and Ripples
TRN	Thalamic Reticular Nucleus
VTC	Ventral Temporal Cortex

1 The Origin of Navigation and Vision Systems

1.1 Introduction: Challenge of Navigation and Vision

The brain's primary purpose is to sense and navigate space for survival. It is due to the simple fact that animals cannot obtain food (= energy source) without motion, unlike plants. To achieve this goal, brains have evolved to perceive and memorize external 3D space under the allocentric (=absolute) frame. Therefore, the internal coordinate system in a brain must be the faithful representation of the external allocentric coordinate system. However, this requirement imposes a formidable challenge on the brain because sensory inputs are always egocentric.

This challenge is even more daunting because, to be exact, sensory signals can only carry information in the time domain due to causality and locality, as discussed in the previous **Part I** (Arisaka 2022). If so, how can animals perceive and represent space internally via neural signal processing? In **Part I**, we introduced a new concept of **MePMoS**, where the frequency-time domain can represent space through sensory-motor integration. The essence is to utilize rhythmic oscillations by CPGs or brainwaves that conduct space-to-time conversion. At the end of **Part I**, we have successfully applied **MePMoS** to construct the entire dynamic connectome of *C. elegans* and human brains.

In this **Part II** of the **Grand Unified Theory of Mind and Brain**, we shall further explore the fierce challenges that animals overcame to navigate space properly. To be more precise, the challenges are fourfold:

1) Internalization of external allocentric 3D space by stamping key landmarks (such as food locations and nests) on it, purely based on egocentric sensing such as vision.
2) Recognition of multiple landmarks with semantic information, regardless of their 3D locations, size (scale), and 3D orientations of [yaw, pitch, roll]
3) Keeping track of one's own 3D position, direction, and speed in real-time within the allocentric frame.
4) Establishing long-term episodic memories of experienced allocentric 3D space to repeat the same navigation in the future.

Below we will investigate how the solutions to these challenges have been addressed by nature from the evolutionary perspective, starting from the very origin of the brain. In this regard, a significant recent breakthrough in understanding insect navigation systems provides critical insight, as *C. elegans* offered in **Part I**. Thus **Section 1** in **Part II** is devoted to the latest discoveries in insects' navigation and vision systems. It is eye-opening to realize that insects overcame most of the above four challenges effectively through evolution. But to begin with, we will first review the most primitive animals with simple diffuse neural networks.

1.2 The Origin of the Brain – Diffuse Nerve Net for Reflexive Behavior

Throughout the introductory **Part I**, we emphasized that space must be represented by time in the brain to perceive it due to causality and locality. As an example, we introduced the *C. elegans* neural system with 302 neurons (Altun et al. 2021) in **Part I: Section 3-4**. Clearly, this simple animal conducts the new concept of **MePMoS** (**Me**mory-**P**rediction-**Mo**tion-**S**ensing) to express external space by time, utilizing rhythmic head/body motions. However, such a strict space-to-time conversion is not always necessary, especially if one's actions in space do not rely on the perception and memory of that space. For example, we already showed how one could obtain the length of a one-foot-long bar only by using the handspan as a unit of length (**Part I: Section 1.3**). Such a measurement technique relies on

uniformly distributed sensors in space with a fixed and known distance between them. These distributed sensors seem to be an efficient alternative to obtain distance, as opposed to involving space-to-time conversion. [*Please note that to be exact, the perception of length by distributed sensors still requires a brainwave that measures the distance between two sensors in the Somatosensory Cortex as shown later in* ***Part V***.]

Indeed, there is an entirely different type of simplest nervous system, the diffuse nerve net. It is a diffuse and scattered neural network system that is homogeneously distributed within a multicellular organism, such as the Hydra and the Jellyfish. This simple nervous system was likely to precede the emergence of the central nervous system (CNS), including the one found in *C. elegans* (Koizumi, 2007).

Recent genetic investigation revealed remarkable similarities between the nerve net and CNS, indicating that the nerve net was indeed the very beginning of primitive brains (Arendt, Marlow, & Tosches, 2016). Even the simplest form of the nerve net, such as Hydra's nerve ring, exhibits some form of a centralized structure (Koizumi 2007; Koizumi et al., 2015). As soon as the organism detects a food source, its nerve ring receives directional stimulation from the outer sensory neurons and reacts by moving in that direction. In other words, the nerve net effectively conducts sensory-motor integration for directional reflexive behavior, exemplifying the brain's primary purpose.

Interestingly, this process enables the internalization of external space without reliance on explicit space-to-time conversion. Later, we will argue that it only produces a reflex instead of the "*conscious perception of space*" that the CNS generates. Nevertheless, it is sufficient for reacting towards stimulation; a reflex causes one-dimensional directional action with the polar coordinate system. Such direct parallel couplings of sensory-motor neurons appear to have been conserved through evolution and served as the basis of prompt parallel processing. Here are a few examples:

1) Snake's forked tongue can detect slight chemical gradients (Schwenk 1994).
2) Rodent's 2D array of whiskers can sense the texture of objects (Petersen 2007).
3) Our five fingers can discern the sizes of hand-size objects (Wiestler, McGonigle, and Diedrichsen 2011).
4) We can conduct directional reflexes via the dorsal visual pathway CIP/VIP/AIP/PMv(F5) → Motor Cortex (Murata, Wen, and Asama 2016),

Let us first investigate this notion that may contradict our previously established argument for the necessity of space-to-time conversion by **MePMoS**. After that, we will consider elements of both processes to develop an innovative concept of "holographic tomography" in the following **Section 2**, which integrates both the concept of **MePMoS** (requiring space-to-time conversion) and the neve-ring-like parallel processing mechanism (without space-to-time conversion).

1.3 The Origin of the Navigation System – Insect's Ring Attractor

Any animal with a nest must recognize its location in the external allocentric frame; only then would the animal be able to return to the nest. Many insects have the well-known ability to go back and forth between their nests and where food is located, such as honeycombs and flowers in the case of honeybees. Recently, the mechanisms behind the navigation systems of various insects have been revealed through extensive research (Fisher et al. 2019; Green et al. 2017; Honkanen et al., 2019; Kim et al., 2019; Pegel et al., 2019; Stone et al., 2017), which opened a new window of our understanding the navigation system at the single neuron level.

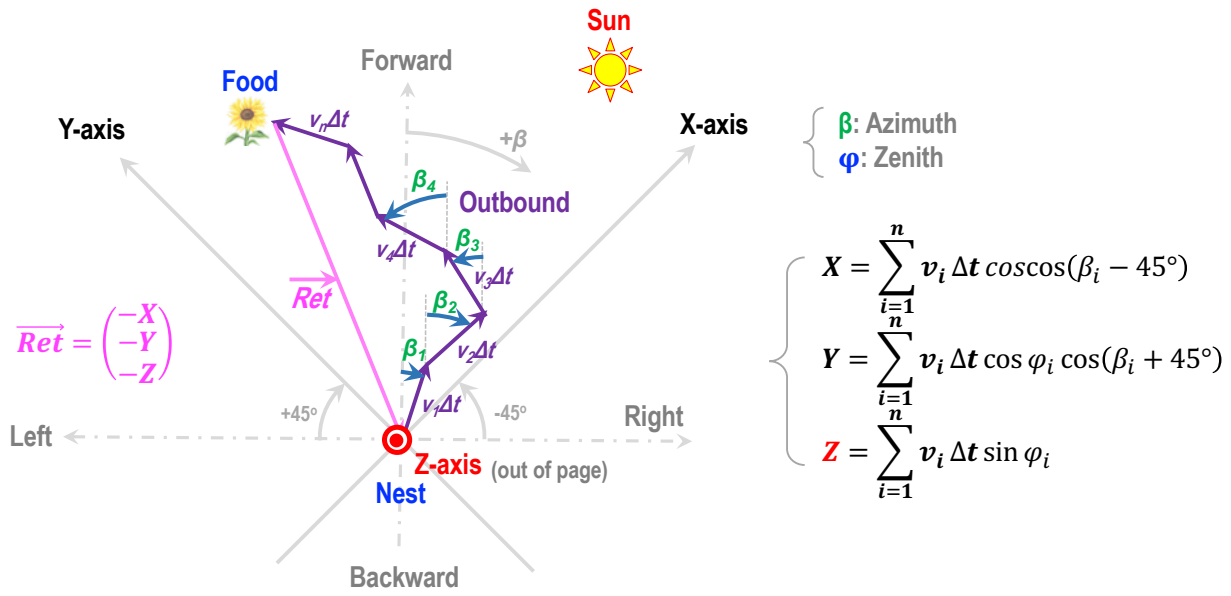

Figure 1. Principle of insect's 3D navigation between the nest and a food location. The direction vector of each step by the polar coordinate is deconvoluted to the (X, Y, Z) components of the 3D Cartesian coordinate system, which are counted by the spike rates. These (X, Y, Z) spike rates are integrated until insects arrive at the food location. The returning vector is given by the opposite direction vector = (-X, -Y, -Z).

The crucial piece in insects' Central Nervous System (CNS) is the ring attractor that consists of multi-layered ring-shaped nerves (Honkanen et al. 2019). Due to its morphological similarity to the primitive diffuse nerve net, it is natural to speculate that the nerve ring within the diffuse nerve net eventually evolved into the ring attractor of insects and other arthropods such as spiders and crustaceans. The ring attractor's critical advantage is its ability to maintain the allocentric head-direction vector regardless of the host's head/body reorientation.

Roughly speaking, the ring attractor consists of double rings that resemble nerve rings. The outer ring receives visual stimulation from the compound eyes through direct mapping. It also receives absolute reference direction from the Sun and optical flow signals. On the other hand, the inner ring, which is interconnected with the outer ring, acts like a gyroscope; it maintains the absolute direction of the Sun so that the allocentric (i.e., geometric) direction is maintained and unchanged.

To maintain allocentric direction by the inner nerve ring, individual neurons in the outer ring must properly remap onto all the neurons of the inner ring by reflecting body motion, rotation, and observed optical flow. Considering 16 neurons (sections) as a typical number per ring, there must be 16 synaptic connections per single neuron in the nerve rings. Thus 16 x 16 = 256 connections are necessary, which is feasible and observed in the insect's ring attractor (Stone et al. 2017).

To keep track of the displacement that results from each movement in allocentric space, insects must obtain their instantaneous speed and direction within the allocentric frame, and the velocity vector must be constructed in real-time spontaneously. Over time, such vectors must be summed up so that the insect can acquire the total displacement vector from the nest to where food is located. This mathematical process is demonstrated in **Figure 1**. That is, with every movement, the velocity vector in polar coordinates (given by the direction and speed) must be deconvoluted into the equivalent x and y components of Cartesian coordinates.

The biological mechanism of this polar-to-Cartesian frame transformation has been recently discovered in two-dimensions (Lyu, Abbott, & Maimon, 2020). They revealed that the Cartesian coordinate system is formed by the two orthogonal axes (marked as X and Y in **Figure 1**) that are tilted from the forward/backward axis by 45 degrees. The convoluted X/Y components are counted by the spike rates measured by the two counter neurons. These counter neurons effectively sum up the velocity vectors associated with each step of movement in (X, Y) directions separately, step by step. Thus, when the insect arrives at the location of food, the homing (returning) vector can be represented by the (-X, -Y) vector.

This discovery is noteworthy, providing the first direct evidence for an animals' ability to convert the egocentric frame (for sensing) to the allocentric frame (for navigation). Furthermore, it converts from the polar coordinate to the Cartesian coordinate system. [*These various coordinate systems will be defined precisely later in* **Section 4**.] The Cartesian system is essential for summing up multiple displacement vectors, as shown in **Figure 1.** This observation naturally leads to the speculation that rodents' hippocampal navigation with place cells and grid cells may share a common biological mechanism. But how can they achieve this frame conversion especially based on vision? We will investigate it later in **Parts III** and **IV**.

Three remarks shall be made before we conclude the discussion of insect navigation. Firstly, in real life, insects must navigate not just in 2D but in 3D, as the nest and the food are not always located on the same horizontal flat 2D plane. To address this problem, **Figure 1** is extended to include 3D navigation with the addition of the Z-axis (directed vertically, going out-of-page). This extension from 2D to 3D would require an additional ring attractor responsible for tracking non-zero azimuth angle (elevation) in real-time. Then, it becomes mathematically feasible to form a 3D direction vector in the 3D polar coordinate system by the yaw and pitch angles, which can be deconvoluted into the corresponding 3D-Cartesian (X, Y, Z) components, as formulated in **Figure 1**.

Secondly, even though their navigation system is so elegantly designed, it appears impossible for insects to visit multiple locations with food during one single round trip and for them to situate these locations that they have memorized onto a navigation map. It is due to the lack of a 2D (or 3D) memory structure to accommodate multiple locations; while they do have X and Y (and probably Z) spike-rate counters (Lyu et al. 2020), there is only one counter for each axis. This limitation leads to our argument of space-to-time conversion being necessary for the evolution towards perception and memory of 3D allocentric space, which we expand upon in the following **Section 2**. Quite interestingly, such evolution had already begun in *C. elegans* (**Part I: Section 3**).

Lastly, suppose insects navigate external space based on spike rate (Lyu, Abbott, and Maimon 2020) rather than alternative mechanisms such as spike timing. In that case, it must be true that they do not consciously perceive space because the spike rates cannot communicate with each other. Furthermore, such a conclusion would indicate that they cannot memorize and recall the space they have previously navigated when trying to repeat a trip. Thus, insects would have evolved to resemble a well-designed robot capable of performing complex reflexes. As such a conclusion seems too extreme and unlikely, further investigation is needed to explore the existence of brainwaves in the insect's navigation system.

Nevertheless, the ring attractor in the insect central brain appears to be among the optimal apparatus for navigation, allowing insects to steer swiftly in a given space with a minimal number of neurons. This perhaps accounts for insects' enormous abundance and success on Earth.

1.4 The Origin of Visual System – Fly's Eyes

We left one essential question unexplained throughout the above argument about the insect navigation system: how the organism recognizes and distinguishes numerous landmarks such as nest,

food (prey), and predators. In this regard, the visual patterns of the landmarks must play a critical role. The fly's vision system has recently been extensively studied (Apitz & Salecker, 2014; Caves et al., 2018; Kolodkin & Hiesinger, 2017; Nériec & Desplan, 2016; Otsuna et al., 2014; Sato et al., 2013). Nevertheless, the actual mechanism of visual perception and memory is still poorly understood, even though roughly 60% of ~250,000 total neurons in the fly's brain appear to be assigned for vision (Nériec & Desplan, 2016).

As we have already discussed, vision does not merely provide a passive perception and recording of an object's image, as one might naïvely guess. First, the retinotopic 2D image by itself is "invisible" unless the corresponding neurons communicate with each other by assigning well-defined time sequences (**Part I: Section 1.5**). Moreover, visual perception and recognition of a landmark require precise one-to-one matching between the sensory input and the already-formed memory. Since one must expect that the image of a landmark would show up at any location in 3D external space, with any size, and with any 3D orientation, the exact external-internal matching of 3D shape of the landmark would require 7D frame translations between the egocentric frame (= sensing) and the allocentric frame (= perception and memory) as already mentioned in **Part I: Section 1.2**.

Until further research directly addresses the stringent requirements above, one could only speculate upon what mechanisms may be involved in insect vision. Intriguingly, 2D retinotopic images retrieved by the approximately 800 independent eyes of the fly are processed by the column structure in the optic lobe, while only highly compressed signals are transferred to the central brain. This image compression procedure appears to resemble what occurs in the human ventral pathway, in which 2D retinotopy in the human's primary visual cortex (V1→ V4) abruptly disappears at the next stage of visual processing in the PIT (Abdollahi et al. 2014). **Section 2.5** argues that this phenomenon constitutes definitive evidence for space-to-time conversion in visual perception (as introduced in **Part I: Section 1.5**) and illustrates the specific universal mechanism involved in this process. The human visual system will be extensively unraveled in **Part III**.

1.5 Summary – Insect's Ring Attractor as the Origin of Brain

In **Section 1**, we discussed a different approach to acting on external space without utilizing CPGs and brainwaves. This alternative neural signal processing is based on so-called ring attractors that are well-established structures within the central nervous system of insects. The one-dimensional circular arrangement of neurons accepts directional sensory visual cues within the egocentric frame, which can be transferred by a matrix of synaptic connections to the internal secondary neural ring that acts like a gyroscope to maintain the allocentric frame.

This remapping from egocentric 1D to allocentric 1D involves parallel processing and instantaneous. That is probably why it has evolved and is conserved in insects' brains as the primary navigation principle. However, such parallel processing cannot generate perception and memory of space by a centralized nervous system. It only creates an unconscious reflex. In this regard, this principle is quite the opposite and contrary to the CPG-based navigation system of *C. elegans* based on the top-down **MePMoS**.

This distinction brings us to an exciting possibility that, perhaps, nature has evolved to take advantage of both principles and somehow combined them. In this regard, it is worth noting that the neural system of *C. elegans* exhibits a few CPG networks that link a series of half-center oscillators by reciprocal inhibition. Such 1D-linear CPG networks could naturally form a ring attractor by connecting the two ends. Once done, such a CPG network could propagate and circulate a brainwave, either clockwise or counterclockwise or perhaps in both directions. We will explore such possibilities in the following **Section 2.**

2 Neural Holographic Tomography (NHT)

2.1 Dimensional Reduction from 2D → 1D (Space) + 1D (Time)

As discussed in **Section 1**, the insect ring attractor is well designed to maintain allocentric 1D direction (i.e., polar angle), which allows the insect to effectively complete the round trip between its nest and the location of food. However, it seems impossible for the insect to develop an accurate allocentric map with multiple landmarks due to its presumed lack of 2D memory for mapping.

It raises an even more significant challenge if the ring attractor is responsible for visual perception. That is because a visual image involves specific shapes whose boundaries contain more than two points. To distinguish a square from a triangle, for example, the visual system must recognize that the square shape has four corners rather than three. Fundamentally, visual perception of a shape requires the construction of a navigation map in visual (vertical 2D) space. Yet, obviously, a simple ring attractor would be able to accommodate patterns of neither shapes nor maps.

There is another challenge shared by navigation and vision. Both navigation and vision must convert the egocentric frame from sensing to an allocentric frame for perception. The ring attractor can only construct and maintain an allocentric direction vector between two points. On the other hand, the transformation of complex navigation maps or visual shapes is basically from 2D → 2D', or even 3D → 3D' mapping.

Let us consider an array-like retina that records a 2D image in the egocentric frame. For simplicity, we will assume that this retina consists of 1000 x 1000 = 10^6 pixels. After a saccade, the next incoming image is abruptly shifted on the retina. However, we do not notice this shift because the new image is properly remapped onto the same allocentric frame that the previous image (before the saccade) was on; moreover, this allocentric frame – rather than the egocentric retinotopic image – is what we consciously perceive. To achieve this prompt 2D → 2D' linear frame translation, each pixel in the initial 2D image must be prepared to be remapped onto any arbitrary location among the 10^6 pixels of the new 2D' image. It means that a total of 10^6 x 10^6 = 10^{12} connections are required, which seems like an impossible mission. The fundamental difficulty lies in the fact that remapping from 2D to 2D' requires 2D x 2D' = 4D synaptic connections.

If one considers the 3D vision that we perceive, the remapping becomes far more exceedingly challenging because it would require 3D x 3D' = 9D synaptic connections. Assuming 100-pixel resolution in the depth direction, 3D would be presented by 1000 x 1000 x 100 = 10^8 pixels (named voxels in 3D); consequently, a total of 10^8 x 10^8 = 10^{16} connections would become necessary, which far exceeds the total number of synaptic connections in a human's entire brain (i.e., ~10^{14}).

Let us focus back on the remapping in 2D for a moment. If one could convolute – or, in a way, "squeeze" – 2D space into 1D space by converting the other 1D space to time, then the remapping (now just 1D → 1D') would only involve 1D x 1D' = 2D synaptic connections. In this case, only 1000 synapses are required per neuron (or pixel), which seems achievable. (Each neuron in the human brain has an order of 1000 synaptic connections). The ring attractor in the insect's central brain is known to conduct 1D → 1D' remapping by 16 x 16 = 256 synaptic connections (**Section 1.3**). Thus, a key of 2D remapping is to reduce the 2D space to 1D space and to convert the other 1D space into the time domain.

There are several established artificial technologies today that utilize this kind of dimensional reduction from 2D (Space) → 1D (Space) + 1D (Time). The most common example is the readout of CMOS image sensors (**Part I**: **Section 1.5**). Here, 1D space (i.e., linear pixels) is converted to a time sequence. The 2D-retinotopy-based vision of any animal – especially human - must have gone through

the realization of a similar 2D → 1D + 1D conversion, which we will show later in **Section 2.3,** and **Part III,** especially for human vision.

2.2 Tomography and Hologram

What about navigation maps, which have no corresponding physical 2D pixels to register space, unlike visual images? In this regard, a similar situation can be found in **Computer Tomography** (**CT**). CT is a well-established medical imaging technique, where the 2D cross-section of an object (such as the human body) is observed by a surrounding ring-shaped 1D detector (such as an X-ray imaging device). With a cylindrical 2D surface detector, a 3D object (such as the entire human body) can be recorded in 2D as well. Offline analysis by a back-projection algorithm allows for restoration of the original 2D cross-sectional view (from 1D) or 3D volumetric view (from 2D) (Willemink & Noël, 2019). Positron Emission Tomography (PET) may be an even better example. With an extra Time-of-Flight measurement (called TOF-PET), the 2D location of a tumor (where metabolism is higher) can be registered by the traveling time of gamma rays from its emitted location to the gamma-ray detector. This TOF measurement is similar to 2D reconstruction by the phase-encoding of brainwaves, as shown in the following **Section 2.3**.

Another approach is by a **Hologram**, initially introduced by Dennis Gabor (Gabor, 1948). In a holographic recording, the depth information of an object is transformed into the phase of coherent optical light on 2D media. Thus, a 3D structure can be kept effectively on a 2D medium. One could broadly define "hologram" as a way of converting spatial information (i.e., distance) to the phase of traveling waves (i.e., temporal difference).

Let's take the example of the klinotaxis of *C. elegans* (Ward 1973), as mentioned earlier (**Part I**: **Section 3.5**). The rhythmic head motion of a worm by its CPG leads to the sensation of NaCl concentration at the sensory neuron. This sensation changes as a function of time by following the head location at a given time. Therefore, the spatial location (where the head is swinging) is converted to the phase of the CPG in time. Clearly, this is based on the broad concept of holography.

The same can be said when humans navigate a dark room by waving our hands left and right (**Part I: Section 2.3**). If our hands are swinging rhythmically, the location of the walls we may touch is presented by the phase of rhythmic hand motion. Therefore, the head location is given by the phase of the hand motion. Since spatial navigation of animals is based on sensory-motor integration by **MePMoS**, it is fundamentally holographic; space must be converted to the phase of the movement.

There is even a clearer-known piece of evidence that is the theta phase precession in the rodent hippocampal system (Skaggs et al., 1996; Jones & Wilson, 2005; Meer & Redish, 2011). Here, the predicted distance to the next landmark is expressed by the phase of the theta brainwave. We will discuss this mechanism in detail in **Part IV**.

All three examples above indicate that, like in tomography and holography, our brain also converts space to time by utilizing the phase of brainwaves. This fundamental principle is the heart of this paper, which we shall name "**Neural Holographic Tomography (NHT)**," as adopted in the title of the article.

2.3 Neural Holographic Tomography (NHT) – 2D Toy Model for 2D Navigation

Let us explore a possible complete mechanism behind space-to-time conversion in the brain, step by step. Cleary both navigation and vision must involve a dimensional reduction of 2D (or 3D) to 1D by space-to-time conversion. To begin with, we will apply this principle to simple 2D navigation. Then we will move on to 3D navigation, 2D vision, then finally 3D vision in this order.

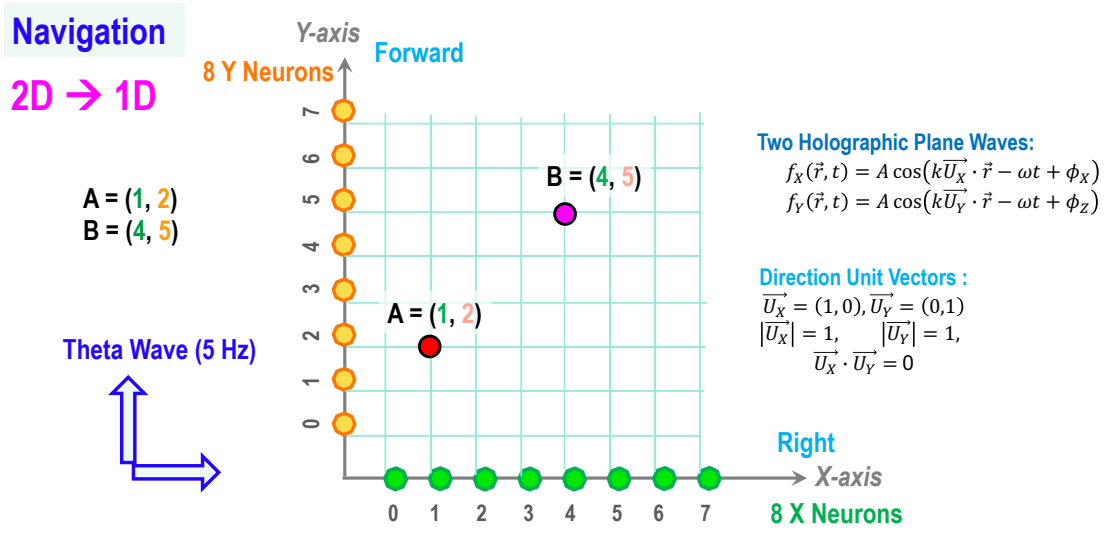

Figure 2. Principle of **Neural Holographic Tomography (NHT).** This demonstrates that two landmarks, A = (1, 2) and B = (4, 5) on the 2D space of (x, y), can be registered by three orthogonal brainwaves, arriving at the 8 X-neurons + 8 Y-neurons for navigation purposes**.**

An appropriate starting point of 2D navigation would be the insect navigation system based on the ring attractor, which has been already explained in **Section 1.3**. To recapitulate, below lists its remarkable achievements.

1) Maintenance of the allocentric frame by the Polar coordinate system (in 2D)
2) 1D (egocentric polar angle) → 1D' (allocentric polar angle) linear translation for conversion of the egocentric frame to the allocentric frame,
3) Further conversion from allocentric polar coordinates to allocentric Cartesian coordinates, and therefore,
4) Locating the insect's absolute (allocentric) position within the Cartesian coordinate system, at least, one position at a given time.

A critical limitation here is the lack of memory to record multiple landmark locations on a single navigation map. To overcome this situation, let us first consider a 2D toy model consisting of two strings of neurons on a horizontal plane: eight X-neurons on the x-axis (to the right) and eight Y-neurons on the y-axis (forward), as shown in **Figure 2**. Here, each line of eight neurons behaves like a ring attractor, but for simplicity, we assume simple straight strings of neurons.

How can two points, A at (1, 2) and B at (4, 5), be perceived and registered, utilizing these 8 + 8 linear neurons to form a 2D navigation map? Here, we shall apply the principle of tomography and holography, which depend on space-to-time conversion based on the phases of brainwaves. Let us assume two orthogonal brainwaves, traveling along with the X and Y directions separately.

[*As shown later in* **Part IV**, *the theta brainwave (with f ~5 Hz) is responsible for navigation in the case of vertebrates* (Buzsáki 2006; Buzsáki 2015; Lisman et al. 2017; Buzsáki 2018).]

The Y (forward) direction of the brainwave travels to the front through the eight Y (forward) neurons with constant speed as a function of time (from Y = 0 at t = 0). As a result, for example, the position of Point A = (1, 2) is projected onto the X = 1 neuron with a Y-phase of 2. Likewise, the position of Point B = (4, 5) is recorded by X = 4 neuron with a Y-phase of 5. [*Here, we assume a special unit: one period = phase shift of 8.*]

Similarly, the X (right) direction of the brainwave goes through the eight X neurons, where the position of Point A is recorded by the Y = 2 neuron with an X-phase of 1, and so on. After all, these processes convert (X, Y) positions to (X-phase, Y-phase) of the brainwaves for both Points A and B, which is the complete expression of space by time in 2D. Through these processes, in principle, any number of landmarks can be effectively encoded and registered holographically and topographically on a 2D map.

This conversion from 2D (space) → 1D (Space) + 1D (Time) is similar to the readout of CMOS image sensors (**Part I: Section 1.5**) or TOF-PET (**Section 2.2**); while keeping 1D space as it is, the other 1D is converted to time (as a phase of brainwave). We argue that this is the fundamental principle of perception of 2D space in time that satisfies causality and locality. The distance between Points A and B is obtained by the phase differences (i.e., time differences) along with the X and Y directions two-dimensionally. Finally, the 2D distance between Points A and B is consciously perceived. After all, this is what Einstein postulated a century ago; the measurement of the distance between Points A and B requires a finite time for a messenger to travel in between, which establishes the "time-like" relation between the two distant points.

We shall name this new principle **Neural Holographic Tomography** (**NHT**); it achieves a **tomography**-like reduction of spatial dimension from 2D to 1D by utilizing the phase of the brainwave to preserve the reduced space information like a **hologram**.

It is worth noting here that, originally, in the case of insect navigation, space is encoded by spike rates; however, in **NHT**, space is encoded by the phases of brainwaves. Therefore, from an evolutionary point of view, conversion from spike rate to spike timing (i.e., phase of brainwave) might have happened, which should be observable. Indeed, such a conversion was found and reported as gamma wave phase shifts in the case of the visual cortex V1, when responding to the orientation of Gabor patterns in cats (Gray & Singer, 1989), and in monkeys (Fries, Nikolić, & Singer, 2007; Vinck, Womelsdorf, & Fries, 2013). Therefore, we assume that such phase coding is a general principle for any type of information processing in the brain. It is simply because, without the conversion from spike rate to spike timing, we cannot perceive or memorize space (**Part I: Section 1.5**).

2.4 The Synaptic Memory of 2D Navigation Space by NHT

The next critical issue to address is how memorization of 2D space occurs in a compact manner; without proper memory, perception is useless for prediction. A key starting point is that, in the **NHT** model, 2D space is already expressed by time (i.e., phase of brainwave) as already explained. Therefore, the well-known concept of Hebbian plasticity plays a fundamental role in memorization by utilizing the exact time conscience.

Let us consider an 8 x 8 matrix of synaptic connections in **Figures 3-A** and **3-B**. **Figure 3-A** shows that the theta brainwave travels through the Y neurons (from 0 to 7) to the forward direction. Then each Y-neuron (at the specific phase) sends out signals along the path of

One Y neuron → 8 axons → 8 synapses → 8 dendrites → 8 X neurons.

As a result, in this specific example, Point A = (1, 2) establishes a new memory of the Y→X synapse of (1, 2) by means of Hebbian plasticity.

On the other hand, **Figure 3-B** shows the opposite direction; the theta brainwave goes through the X neurons (from 0 to 7) to the right. Then each X-neuron (at the specific phase) sends out signals along the path of

One X neuron → 8 axons → 8 synapses → 8 dendrites → 8 Y neurons.

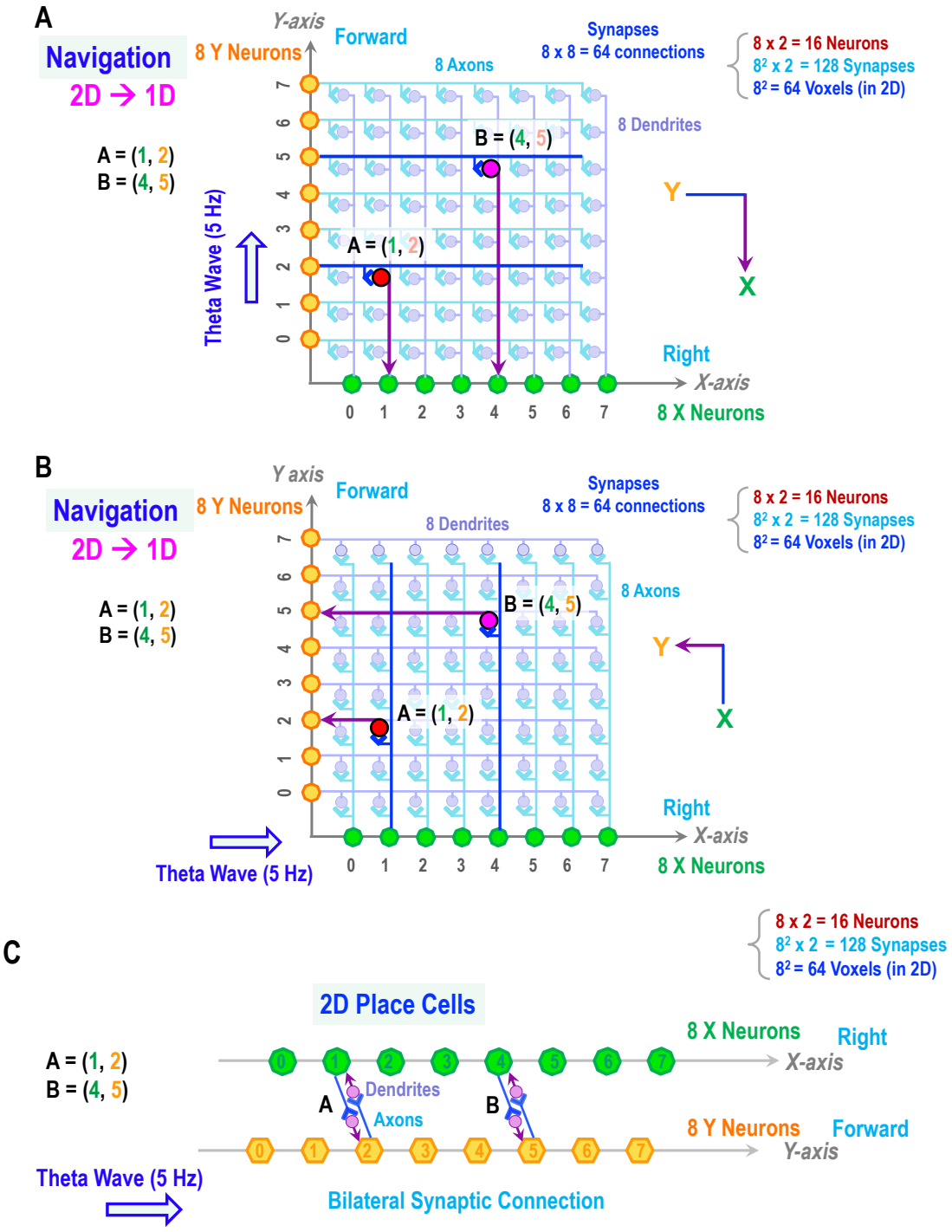

Figure 3. Principle of **Neural Holographic Tomography (NHT).** **(A)** and **(B)** show 8 x 8 = 64 synapses that record 8x8 = 64 locations in (X, Y). **(A)** shows that each Y neuron sends out signals along the path of 8 axons → 8 synapses → 8 dendrites → 8 X neurons, whereas **(B)** goes the opposite direction, starting from eight X neurons and arriving at eight Y neurons. Two landmark points: A =(1, 2) and B = (4, 5) are connected by four synapses marked "red". **(C)** is equivalent to (A) and (B), but it demonstrates a compact arrangement of the memory unit established by the four synaptic connections.

This time, Point A = (1, 2) is connected by the X→Y synapse of (1, 2). To the end, Point A = (1, 2) is physically connected and memorized by the two synapses through Hebbian plasticity. Together with B = (3, 4), a total of four synapses are marked "red" in **Figure 3-A, B**. Lastly, **Figure 3-C** is equivalent to (A) and (B), but it demonstrates a compact arrangement of the memory unit established by the four synaptic connections. We will gradually develop this idea to define the "*engram*."

[*The conceptual idea of the engram is reviewed by several articles:* (Schacter, Eich, & Tulving 1978; Josselyn 2010; Josselyn & Tonegawa 2020; Eichenbaum 2016).]

In summary, through the perception of 2D navigational space by traveling brainwaves, the synapses corresponding to the actual locations are conveniently rewarded by the precise timing of the assigned phase. Thus, thanks to Hebbian plasticity, the 2D "holographic" space is effectively recorded by the static 2D "synaptic" space. This process is summarized in the box below:

2D navigation space	(8 x 8 = 64 points)
→ **Neural Holographic Tomography** (**NHT**) by brainwaves	(8 + 8 = 16 neurons, 8 + 8 = 16 phases)
→ 2D static memory of landmarks	(8 x 8 x 2 = 128 synapses)

This two-step conversion from 2D space to 2D synaptic memory possesses several unique features. First, it indeed forms a long-term static memory, very much like an SSD memory of today's computer. Second, once it is hard-wired, the established connection is independent of the brainwave (frequency and phase) that generate it. Therefore, the memory can be retrieved by a different brainwave with any preferred frequency and phase. This flexibility of read-out will open a unique feature of arbitrary 2D → 2D' linear frame translation. A perfect example is that a static memory can be based on the allocentric frame, but when it is retrieved by a brainwave, a different phase can be assigned corresponding to the egocentric frame of sensory stimulation. As already discussed in **Part 1: Section 5.5**, such a phase shift is conducted by the PN network by taking corollary discharge into account (Bridge, Leopold, and Bourne 2016)(Soares et al. 2017).

It is worth noting that the above synaptic memory can be considered as the origin of so-called place cells (O'Keefe 1976), which will be discussed extensively in **Part IV**. Basically, a static episodic memory of the allocentric frame for key landmarks can be formed by this mechanism known as place cells. During navigation in the same space for the second time, the current location of the host animal is kept updated by the proper phase shift, resulting in the observed theta phase precession for the nearby landmark.

So far, the above 2D → 2D' linear frame translation is achieved by shifting the phase of brainwaves. What would happen if the readout frequency is higher than the recording frequency, say, by a factor of two. Then the perceived space will shrink by the same factor two due to halving the traveling time. These two degrees of freedom, parallel translation by the phase shift and scaling by frequency change, offer possible machinery of direct matching between the memory (in the allocentric frame) and the sensory input (in the egocentric frame). Through this biological neural process in the frequency-time domain, the concept of **MePMoS** for navigation can be realized.

2.5 3D Toy Model for 3D Navigation

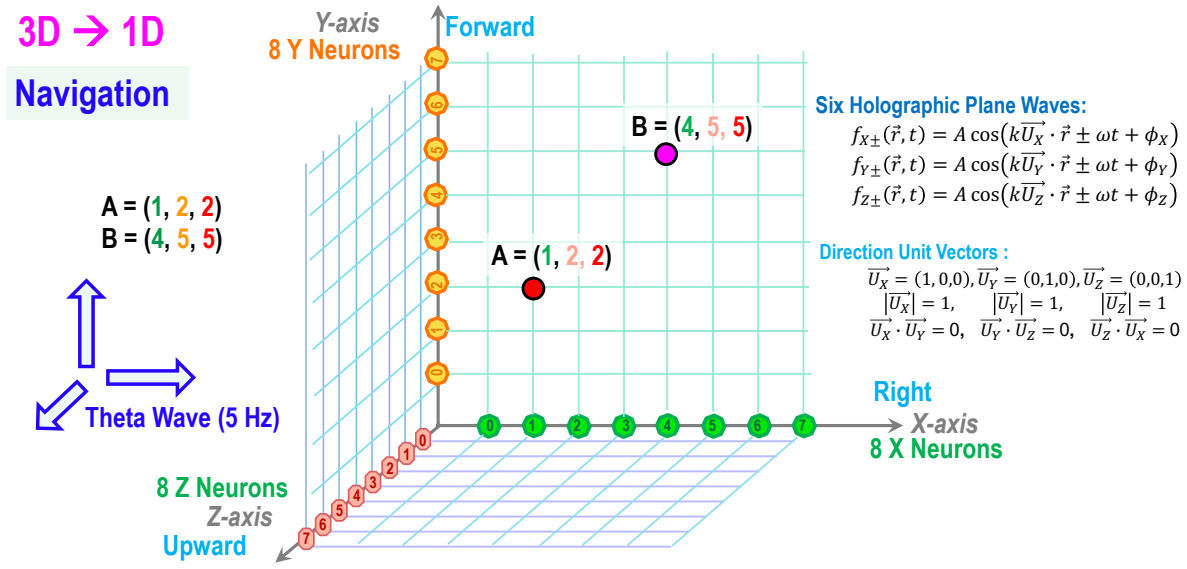

Figure 4. Principle of **Neural Holographic Tomography (NHT)** in 3D navigation. This is a natural extension of the 2D navigation space in **Figure 2**. It demonstrates that two landmarks, A = (1, 2, 3) and B = (4, 5, 5) on the 3D space of (x, y, z), can be registered by three orthogonal theta brainwaves, arriving at 8 X-neurons + 8 Y-neurons + 8 Z-neurons for navigation purposes**.**

The above argument of 2D perception and synaptic memory can be naturally extended to the 3D space. Let us consider 3D space for navigation shown in **Figure 4**. Here, the third axis, Z axis is added for the vertically-upward direction. This time, three brainwaves traveling along with the orthogonal X, Y, and Z directions as shown here. The Y (forward) direction plane brainwave goes through the eight Y (forward) neurons as a function of time step by step from 0 → 7. As a result, for example, the position of Point A at (1, 2, 2) is recorded by both X = 1 neuron and Z = 2 neuron holographically with a Y-phase of 2. Likewise, the position of Point B at (4, 5, 5) is recorded by the X = 4 neuron and Z = 5 neurons with a Y-phase of 5.

Similarly, the X (horizontally right) direction of the plane brainwave arrives at eight X (right) neurons step by step from 0 → 7, where the position of Point A is recorded by the Y = 2 neuron and Z = 2 neuron with an X-phase of 1, and so on. Lastly, the Z (upward) direction plane brainwave arrives at eight Z (right) neurons step by step, where the position of Point A is recorded by the X = 1 neuron and Y = 2 neurons with a Z-phase of 2.

After all, these processes convert (X, Y, Z) positions to (X-phase, Y-phase, Z-phase) of the theta brainwaves for both Points A and B. That is the complete expression of 3D locations by time. In principle, any number of landmarks can be encoded and perceived, holographically and topographically on a 3D navigation map. And this must be the origin of "3D place cells" on allocentric 3D space, to be discussed in **Part IV**.

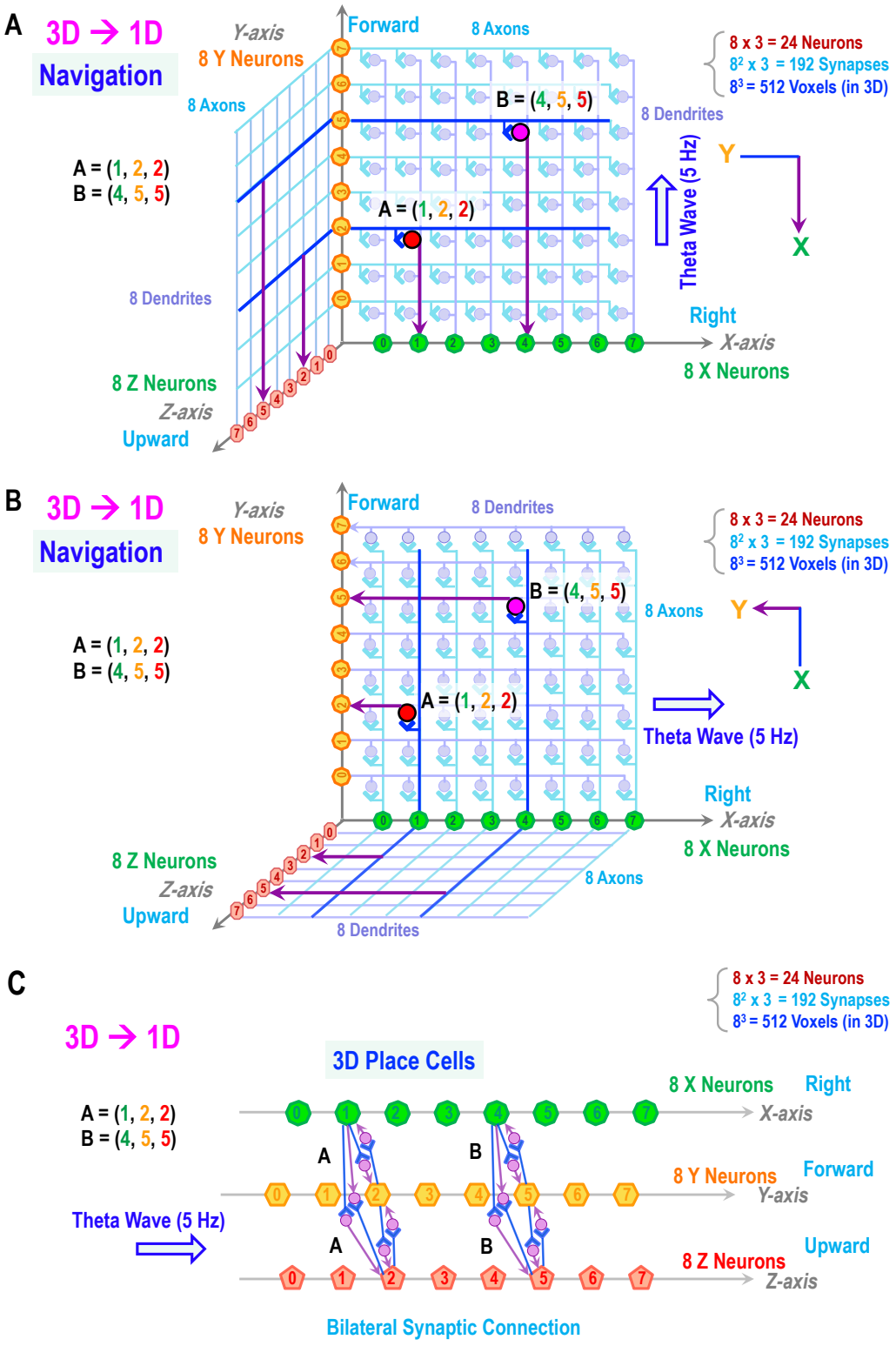

Figure 5. 3D toy model of 3D navigation. **(A)** and **(B)** shows 8 x 8 x 3 = 192 synapses that record 8 x 8 x 8 = 512 locations in (X, Y, Z). **(C)** is equivalent to (A) and (B), but it demonstrates a compact arrangement of the memory unit established by the six synaptic connections.

How can 3D space be memorized? Again, the key starting point is that 3D space is already expressed by the three phases of brainwaves. Let us consider an 8 x 8 matrix of synaptic connections between eight X-neurons and eight Y-neurons in **Figures 5-A** and **B**, which is identical to **Figures 3-A** and **B** so far. But for 3D memory, we introduce additional two sets of 8 x 8 synaptic connections on the (Y, Z) plane shown in **Figure 5-A** and on the (X, Z) plane in **Figure 5-B**.

In **Figure 5-A**, a plane theta brainwave travels to the Y (forward) direction at a constant speed. When it arrives at Y = 2, Y → X is synaptically connected at (X, Y) = (1, 2). At the same time, Y → Z is synaptically connected at (Y, Z) = (2, 2). As a result, three neurons, (X, Y, Z) = (1, 2, 2), are linked by the combinations of two synapses: (X, Y) = (1, 2) and (Y, Z) = (2, 2).

Likewise in **Figure 5-B**, another plane theta brainwave travels to the X (right) direction. When it arrives at X = 1, X → Y is synaptically connected at (X, Y) = (1, 2). At the same time, X → Z is synaptically connected at (X, Z) = (1, 2). As a result, three neurons, (X, Y, Z) = (1, 2, 2), are linked by the combinations of two synapses: (X, Y) = (1, 2) and (X, Z) = (1, 2).

Lastly, the third plane theta brainwave travels to the Z (upward) direction (which is not shown here). When it arrives at Z = 2, Z → X is synaptically connected at (X, Z) = (1, 2). At the same time, Z → Y is synaptically connected at (Y, Z) = (2, 2), resulting in the two synapses: (X, Z) = (1, 2) and (Y, Z) = (2, 2).

The net result is the mutual six connections of three neurons, (X, Y, Z) = (1, 2, 2), linked by three pairs of (X, Y) = (1, 2), (Y, Z) = (2, 2), and (X, Z) = (1, 2) by biliteral directions, which is illustrated in **Figure 5-C**. Finally, a complete static memory of the 3D location of Point A (X, Y, Z) = (1, 2, 2) is realized by six synapses, forming "3D place cells". The same can be applied to Point B = (4, 5, 5) as well. This process is summarized in the box below:

3D navigation space	(8 x 8 x 8 = 512 locations)
→ **Neural Holographic Tomography** (**NHT**) by three theta waves	(8 + 8 + 8 = 24 theta phases)
→ 3D memory of landmarks	(8 x 8 x 2 x 3 = 384 synapses)

To our best knowledge, this is the first definitive explanation of the origin of **Place cells** "in 3D". It is the outcome of **Neural Holographic Tomography** (**NHT**), converting the 3D → 1D utilizing the three theta brainwaves. It is synaptically connected by Hebbian plasticity, and the corresponding 3 x 2 = 6 neurons will flash altogether when the host animal arrives on top of the place coded by the place cells. This principle can also explain the observed theta phase precession; The distance to the next place in 3D is expressed holographically by the three phases of the theta brainwaves along with three directions in (X, Y, Z). More details of the place cells will be given in **Part IV**.

3 Neural Holographic Tomography (NHT) of 3D Vision

3.1 2D Toy Model for 2D Vision by NHT

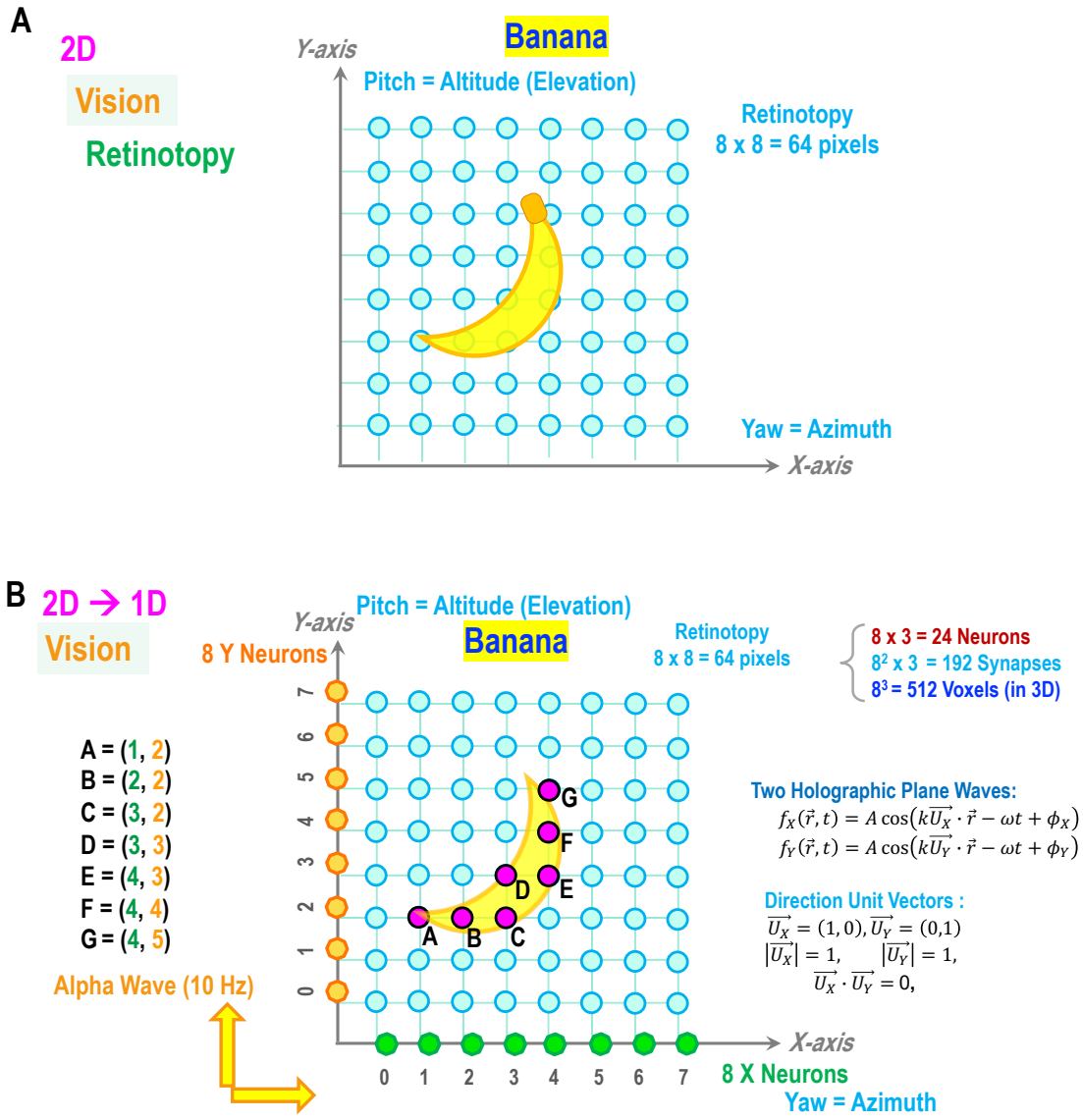

Figure 6. Principle of **Neural Holographic Tomography (NHT)** applied to 2D visual perception. In the case of 2D vision, (X, Y) corresponds to [yaw, pitch] in the Polar coordinate system. It shows a retinotopy by 8x8 =64 pixels, observing a banana-like shape at the center. A total of eight points (A-G) can be recorded by brainwaves, detected by the 8 X-neurons + 8 Y-neurons.

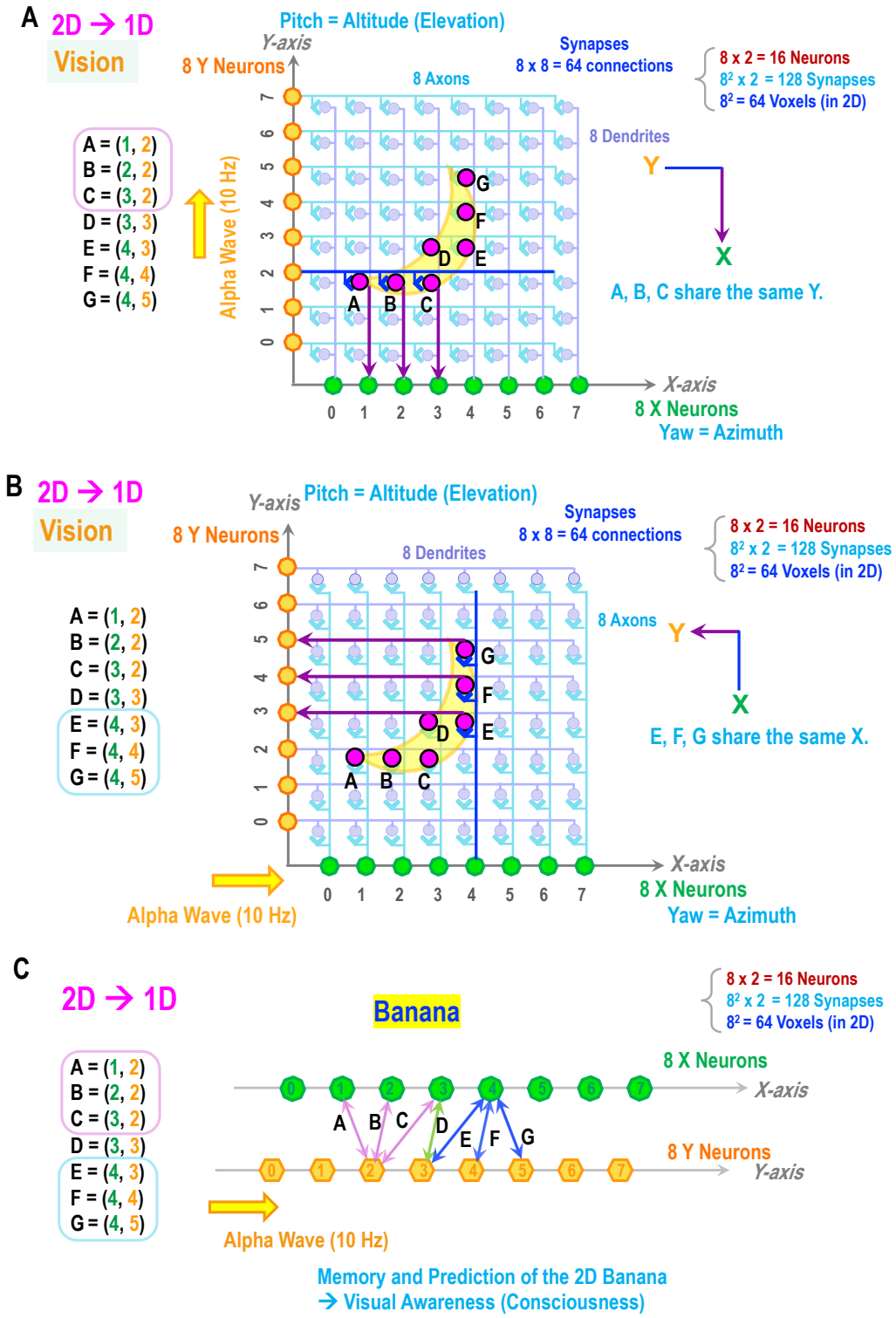

Figure 7. Principle of **Neural Holographic Tomography (NHT)** applied to 2D vision. **(A)** and **(B)** show 8x8 = 64 synapses that record 8x8 = 64 locations in (X, Y). **(C)** shows the image of a banana recorded by a total of 7 x 2 = 14 synapses. The concept is similar to **Figure 3-C**, but the mutual synaptic connections are simplified by a single arrow in both directions.

The new concept of **NHT** can be equally applied to the visual perception of 2D/3D space and shape. Here, we shall start with the visual perception of a 2D banana shape, illustrated in **Figure 6-A**. This time, the horizontal axis, X-axis, is still to the right, but the vertical axis, Y-axis goes vertically upward. Thus, the (X. Y) plane represents the vertically flat plane viewed by eyes.

Let's assume that a retina is composed of 8 x 8 = 64 pixels (= photoreceptors like cones and rods) for simplicity. The 2D retinotopic image of the banana is represented by the seven pixels (as Points A-G) in **Figure 6-B**, which is still "invisible" because these seven pixels are not communicating with one another. In other words, these neurons on the retina are still "space-like" in Einstein's language.

In human vision, a visual pattern of a banana, once recorded onto a 2D retina, is transferred to LGN → V1 → V2 and so on (Felleman and Essen 1991; Gilbert and Li 2013; DiCarlo, Zoccolan, and Rust 2012; Kruger et al. 2013). But this banana shape is still "invisible" through this process. Only after the retinotopic image is scanned by traveling brainwaves and the corresponding neurons start to flash in a well-defined time sequence, they become "time-like", and the image of the banana is consciously perceived. In the case of the human visual pathway, alpha brainwaves ($f \sim 10$ Hz) must play this role of space-to-time conversion (Lozano-Soldevilla and VanRullen 2019), as shown in **Figures 6** and **7**. The space-to-time conversion is expected to happen from V4 to PIT where the retinotopic image abruptly disappears (Abdollahi et al. 2014). [*A more complete description will be given in **Part III**, but the exact biological mechanism of how 2D retinotopy is scanned by brainwaves requires further investigation.*]

Figures 6 and **7** are like **Figures 2** and **3** for navigation, except we consider the continuous seven points for the banana pattern: from A = (1, 2) to G = (4, 5). In the case of vision, let us define the X-axis as the horizontal direction (= yaw angle) and the Y-axis as the vertical direction (= pitch angle). For simplicity, we shall treat them as if they form the 2D Cartesian coordinate system for the time being. In **Figure 6**, the vertical direction (= pitch) of the alpha brainwave travels upwards through the eight Y (vertical) neurons as a function of time. Then, the position of Point A is expressed by the X=1 neuron holographically with a Y-Phase of 2. Similarly, the horizontal direction (= yaw) of the brainwave travels through the eight X neurons step by step, where the position of Point A is expressed by the Y=2 neuron with an X-Phase of 1. In the end, these processes convert the position of (X, Y) in space to time given by (X-phase, Y-phase) of the alpha brainwaves for all seven points: A, B. C… G. That is the complete expression of the 2D banana shape by time. Through these processes, in principle, any 2D shape can be expressed holographically and tomographically, resulting in conscious visual perception.

The next step is to memorize the 2D banana shape in a compact manner. Again, a starting point is that the 2D banana shape has been already expressed by the phases of alpha brainwaves. Let us consider an 8 x 8 matrix of synaptic connections in Figures **7-A** and **7-B**. **Figure 7-A** shows that each Y neuron sends out signals to 8 axons → 8 synapses → 8 dendrites → 8 X neurons, whereas **Figure 7-B** goes the opposite direction from 8 X neurons → … → 8 Y neurons. Through the perception of 2D shape by the traveling alpha brainwaves, each synapse is conveniently rewarded at the precise timing of the assigned phase. Thus, thanks to Hebbian plasticity, the 2D "holographic" image is effectively recorded by the static 2D "synaptic" memory.

Finally, we can derive the physical connection of two strings of neurons in **Figure 7-C** analogous to **Figure 3-C**. But in this case, mutual synaptic connections are simplified by a single arrow in both directions. What is intriguing here is that the horizontal three pixels (A, B, and C) are grouped by sharing the same Y=2 neuron, whereas the vertical three pixels (E, F, and G) are grouped by sharing the same X=4 neuron. Such local groupings are expected to provide tightly connected local patterns of synaptic links.

In summary, through the visual perception of 2D shape by traveling alpha brainwaves, the synapses corresponding to the actual banana shape are conveniently rewarded by the precise timing of the assigned phases. This must be the general principle behind our static long-term memory of 2D visual shapes like human faces, cars, etc. This two-step process of forming 2D memory is summarized in the box below:

"Invisible" 2D Retinotopy	(8 x 8 = 64 neurons)
→ "Visible" **Neural Holographic Tomography** (N**HT**)	(8 + 8 = 16 neurons, 8 + 8 = 16 phases)
→ "Invisible" 2D Memory	(8 x 8 x 2 = 128 synapses)

3.2 3D Toy Model for 3D Vision

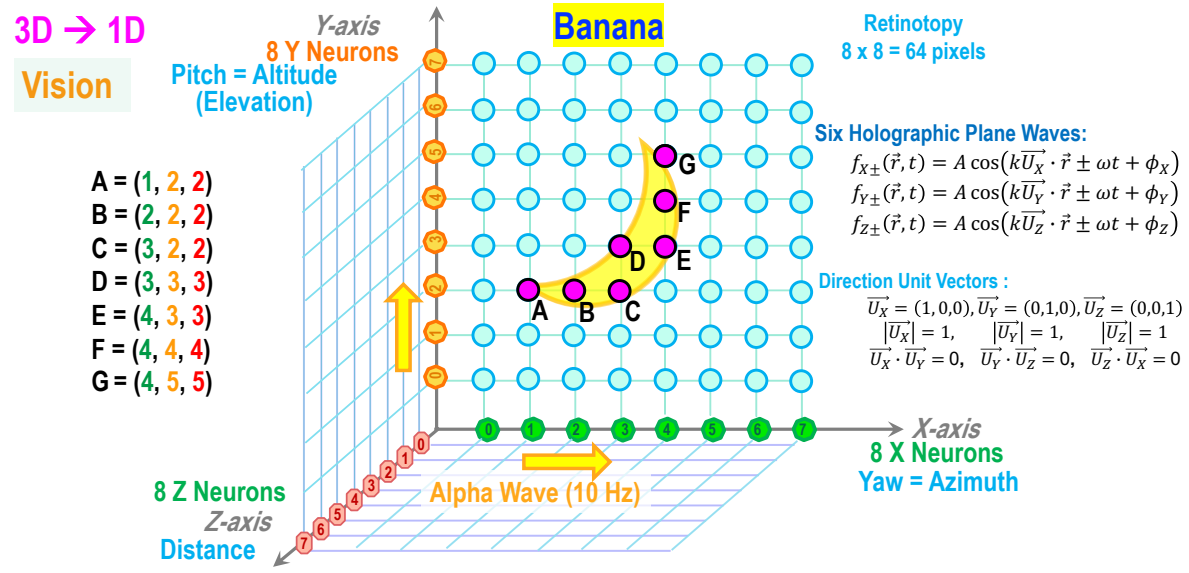

Figure 8. Principle of **Neural Holographic Tomography (NHT)** in 3D vision. This is a natural extension of the 2D vision in **Figure 7**.

In our daily life, we experience visual perception in 3D, even though the initial image on the retina is 2D. How can we obtain such a vivid sensation of depth? The solution to this question can be derived naturally from the new concept of **Neural Holographic Tomography (NHT)**. The complete treatment requires the full description of the detailed visual pathways, which will be given in the following **Part III**. Here, we shall introduce only the basic principle.

As we extended the **NHT** from 2D navigation to 3D in **Section 3.1**, the argument of 2D vision can also be extended to 3D vision. Let us consider the 3D image in Figure 8, where the third axis, Z-axis, is added for the forward direction. [*Please note that Y-axis and Z-axis are swapped compared to Figure 4 for 3D navigation.*]

This time, we shall explore the visual perception and memory of a 3D banana shape, shown in **Figures 8** and **9** (which are analogous to the 3D navigation model in **Figures 4** and **5**.) Here, a 3D banana shape is situated in front of us with a certain distance, occupying the 7 points from A = (1, 2, 2) to G = (4, 5, 5), representing [yaw, pitch, distance] (in arbitrary units). Here, three points, A, B, C are lined up as a horizontal bar, at the same pitch (elevation) Y = 2, and at the same distance Z = 2. On the other hand, another three points, E, F, G share the same yaw (azimuth) X = 4, but slanted away vertically, like E = (4, 3, 3), F = (4, 4, 4), G = (4, 5, 5).

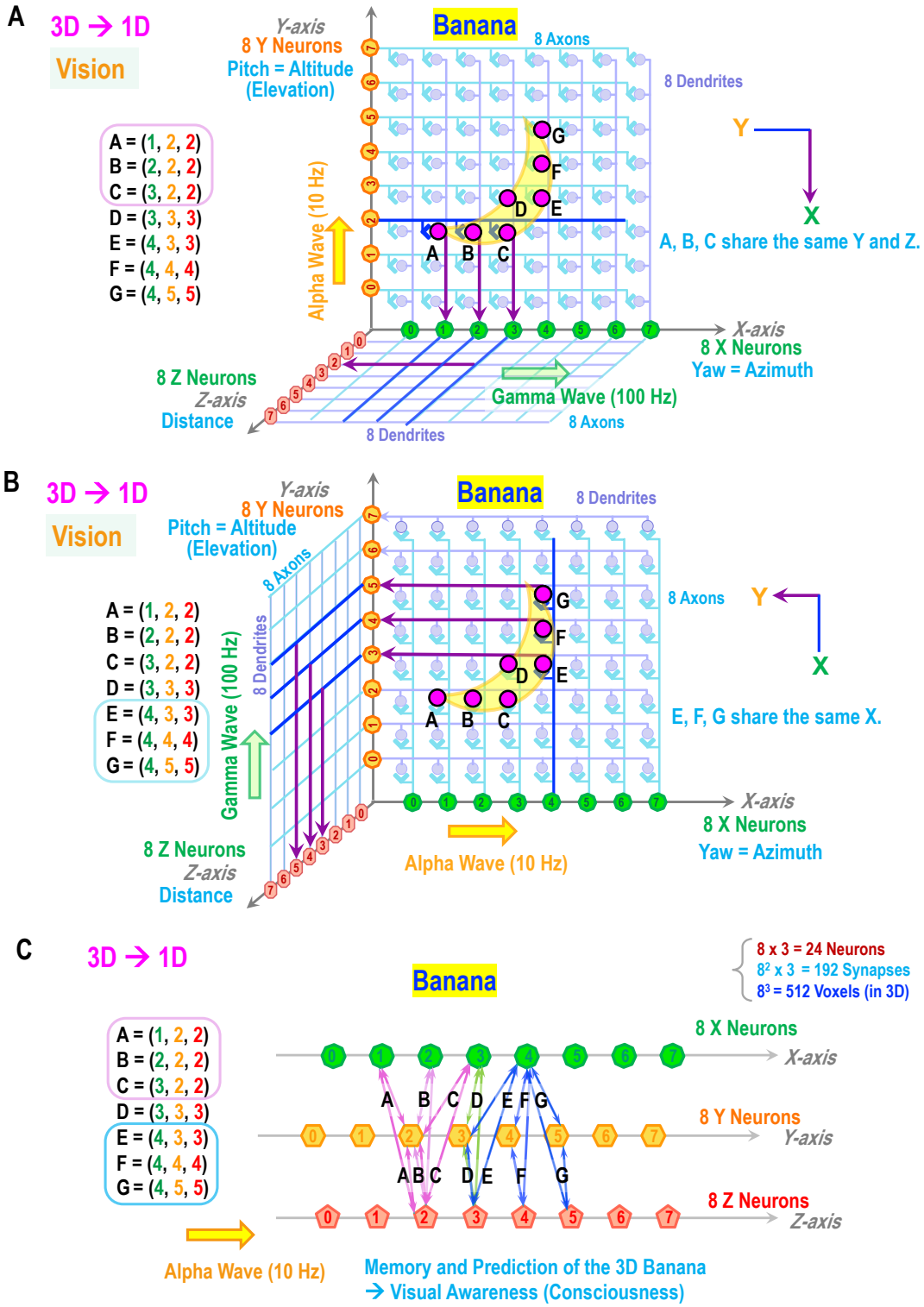

Figure 9. 3D Toy model for 3D vision analogous to the 3D navigation model **in Figure 5**. **(A)** and **(B)** show 8 x 8 x 3 = 192 synapses that record 8 x 8 x 8 = 512 locations in (X, Y, Z). **(C)** is equivalent to (A) and (B), but it demonstrates a compact arrangement of the memory unit established by the 7 (points) x 3 (combinations) x 2 (dual directions) = 42 synaptic connections.

Let us address two fundamental questions. Firstly, why and how can we perceive the banana in front of us at a certain distance? That is, why is the image not located on our retina or within our brain in conscious visual sensation? Then, the second question is why and how can we observe a 3D banana shape with the given slanted angle?

The first question is philosophically profound, but so far, no clear answer has yet been provided by vision research. According to **NHT**, depth perception is given holographically by assigning the specific phases of the traveling brainwave along the depth direction at each given point in a 2D retinotopy image. That is literally "*holographic*". Thanks to the holographic expression of the depth, the 3D location of the banana and its 3D curved shape will naturally appear in our visual perception. [The details mechanism will be proposed in **Part III: Section 4.3**.]

To elaborate on this principle, let us consider three traveling brainwaves along the orthogonal X, Y, and Z directions as shown in **Figures 8** and **9**, which is analogous to the 3D navigation in **Figures 4** and **5**. In **Figure 9-A**, the Y (upward) direction of the plane alpha brainwave is recorded by the eight X (right) neurons and the eight Z (upward) neurons as a function of time. For example, the position of Point A at (1, 2, 2) is recorded by the Y=2 neuron holographically with an X-phase of 1. But what about the depth information of Z=2? Here, unlike the case of the 3D map in **Figure 5**, a different high-frequency gamma brainwave is required for the Z (depth) direction. This is because more than one point, such as A, B, and C, flash together at the same phase of the horizontal plane alpha brainwave at Y= 2, but these three points must be distinguished by the independent timing for encoding possibly different depths (Z).

As a result, the above processes convert the 3D banana shape, given by the seven points from A to G, initially detected by (X, Y, Z) = [yaw, pitch, roll], to the seven sets of (X-phase, Y-phase, Z-phase) of the brainwaves. That is the complete expression of 3D visual perception by time. In principle, any 3D shape can be encoded and registered holographically and tomographically. And this is the true origin of 3D visual perception; we visually perceive 3D space and shape by assigning three times (= phases of brainwaves) at all the observed points. We argue that this is the only way to satisfy causality and locality in our visual pathway and construct the 3D image in front of us.

Lastly, how can we memorize the 3D visual image like a banana shape? Once again, the key starting point is that the 3D image is already expressed by the three phases of brainwaves. Let us consider an 8 x 8 matrix of synaptic connections between eight X-neurons and eight Y-neurons in **Figures 9-A** and **B**, which is identical to **Figures 5-A** and **B** so far. But for 3D memory, we introduce two additional sets of 8 x 8 synaptic connections on the (Y, Z) plane shown in **Figure 9-A** and on the (X, Z) plane in **Figure 9-B**. The rest of the story is the same as the explanation of **Figures 5-A** and **B**, except the depth (Z) direction must be encoded not by alpha but by gamma brainwaves.

The net result is the six mutual synaptic connections of three neurons for every seven points. For example, Point A, (X, Y, Z) = (1, 2, 2), is memorized by three pairs synapses: (X, Y) = (1, 2), (Y, Z) = (2, 2), and (X, Z) = (1, 2) in biliteral directions, which is illustrated in **Figure 9-C**. Finally, a complete static memory of the 3D banana shape, consisting of seven Points A-G, is realized. This two-step process is summarized in the box below:

3D visual shape	(8 x 8 x 8 = 512 locations)
→ **Neural Holographic Tomography** (**NHT**) by three brainwaves	(8 + 8 + 8 = 24 phases)
→ 3D static memory of 3D shape	(8 x 8 x 2 x 3 = 384 synapses)

To the best of our knowledge, this is the first definitive explanation of the origin of 3D visual perception and its memory. Once again, this result is the direct outcome of **Neural Holographic Tomography** (**NHT**), converting the 3D → 1D utilizing three brainwaves. More details of our vision will be given in **Part III**.

It is worth noting that, although we have introduced and utilized the two types of brainwaves: alpha for X and Y directions and gamma for Z (depth) direction, once the synaptic memory is formed, it is static and totally independent of the brainwaves that have established the synaptic connections. The same can be said for the 3D navigation map by the theta brainwave. In other words, 3D memories for vision and for navigation are totally unified, realizing one of the **Grand Unifications**, which leads to the concept of the "*engram*" for both 3D vision and 3D navigation.

3.3 3D Linear Frame Translation by NHT – Overt and Covert Attention

So far, we have shown that **NHT** can elegantly explain the basic principles of navigation and vision universally in both 2D and 3D. Thanks to the space-to-time conversion by brainwaves, well-known Hebbian plasticity can take place and play a critical role to establish static synaptic memories by two (or three) strings of 1D neurons. The **NHT**-based two-step process for memory formation allows establishing the allocentric frame in our memories, even though sensory stimulation enters an Egocentric frame. The best example is place cells, discovered in rodents' 2D navigation. We successfully generalized this concept to 3D navigation by "*3D place cells*" **in Section 2.5**.

This time, let us examine the remaining big mystery of our vision; why and how can we perceive stable external "allocentric" 3D space regardless of constant saccadic eye movements? At this point, it seems straightforward to speculate that allocentric visual perception shares the same principle as allocentric navigation; place cells are anchored in allocentric space. Likewise, visually-perceived images of objects must be anchored in allocentric visual space.

As already discussed in the previous **Sections 3.1** and **3.2**, a banana shape is memorized by synaptic connections between two strings (or three srings) of neurons in the case of 2D (or 3D) vision. Let us take a 3D static memory in **Figure 10-A** and **B** formed for a 3D banana shape, once observed at the fovea center. Assume that we see the same banana again for the second time but at a different location. As shown in **Figure 10-C** and **D**, this time, the retinotopic image is slightly shifted horizontally to the right by two pixels:

A = (1, 2, 2) → A' = (1**+2**, 2, 2) = (3, 2, 2)
B = (2, 2, 2) → B' = (2**+2**, 2, 2) = (4, 2, 2)
…

As a result, the center of the banana, D = (3, 3, 3), which used to be at the fovea center, is now displaced to D' = (3**+2**, 3, 3) = (5, 3, 3). In our daily life, to recognize the banana shape and location, we naturally apply one of two actions: either we move our eyes by an unconscious saccade called overt attention, or we try to identify it without a saccade by covert attention. Overt attention is illustrated in **Figure 10-E**, whereas covert attention is shown in **Figure 10-F**.

Among these, let us start with overt attention in **Figure 10-E** as it directly follows the concept of **MePMoS** through the principle of **NHT**. Overt attention re-allocates the center of the banana D' = (5, 3, 3) to the fovea center D = (3, 3, 3). Consequently, we observe the banana at the fovea center in the egocentric frame, which is essential to recognize the banana shape by overlapping the observed form onto the memorized banana shape. But this image shift is undetected in our conscious visual perception. Why? It is due to the corollary discharge that compensates for our eye movement in real-time. This is conducted by the alpha phase shift from X (egocentric) → X' = X+2 (allocentric), as shown in **Figure 10-E**. Thus, overt attention allows us to extract the semantic shape of the banana in the newly centered egocentric frame while maintaining unchanged the conscious perception of the 3D allocentric frame; we observe the banana at the same allocentric location even after eye movements.

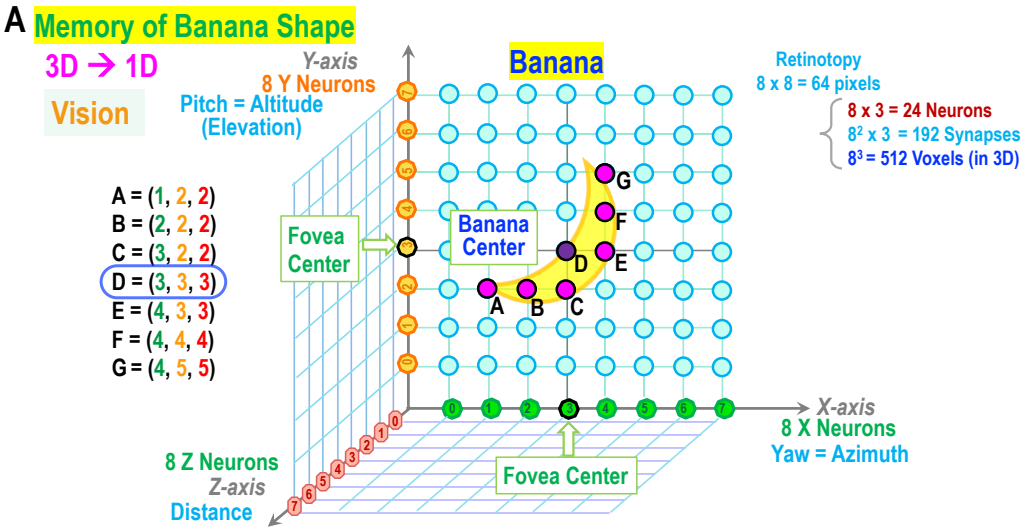
A Memory of Banana Shape
3D → 1D
Vision
Y-axis
8 Y Neurons
Pitch = Altitude
(Elevation)
Banana
Retinotopy
8 x 8 = 64 pixels
8 x 3 = 24 Neurons
8² x 3 = 192 Synapses
8³ = 512 Voxels (in 3D)
A = (1, 2, 2)
B = (2, 2, 2)
C = (3, 2, 2)
D = (3, 3, 3)
E = (4, 3, 3)
F = (4, 4, 4)
G = (4, 5, 5)
Fovea Center
Banana Center
X-axis
8 X Neurons
Yaw = Azimuth
8 Z Neurons
Z-axis
Distance
Fovea Center

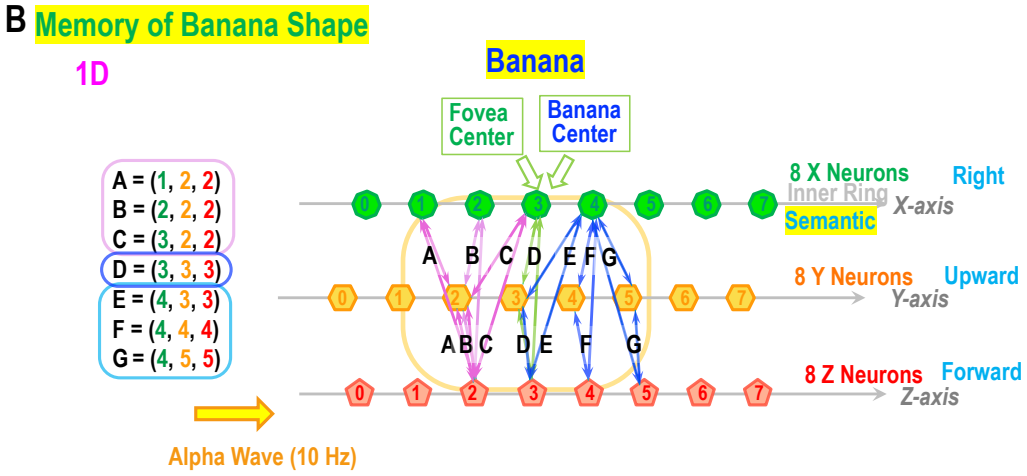
B Memory of Banana Shape
1D
Banana
Fovea Center
Banana Center
A = (1, 2, 2)
B = (2, 2, 2)
C = (3, 2, 2)
D = (3, 3, 3)
E = (4, 3, 3)
F = (4, 4, 4)
G = (4, 5, 5)
8 X Neurons
Inner Ring
Semantic
Right
X-axis
8 Y Neurons
Upward
Y-axis
8 Z Neurons
Forward
Z-axis
Alpha Wave (10 Hz)

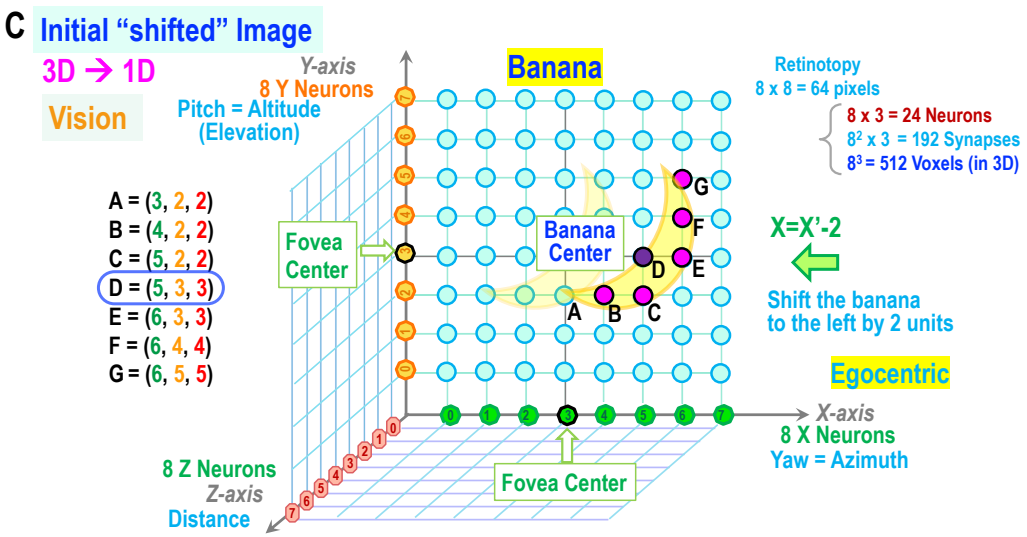
C Initial "shifted" Image
3D → 1D
Vision
Y-axis
8 Y Neurons
Pitch = Altitude
(Elevation)
Banana
Retinotopy
8 x 8 = 64 pixels
8 x 3 = 24 Neurons
8² x 3 = 192 Synapses
8³ = 512 Voxels (in 3D)
A = (3, 2, 2)
B = (4, 2, 2)
C = (5, 2, 2)
D = (5, 3, 3)
E = (6, 3, 3)
F = (6, 4, 4)
G = (6, 5, 5)
Fovea Center
Banana Center
X=X'-2
Shift the banana
to the left by 2 units
Egocentric
X-axis
8 X Neurons
Yaw = Azimuth
8 Z Neurons
Z-axis
Distance
Fovea Center

D

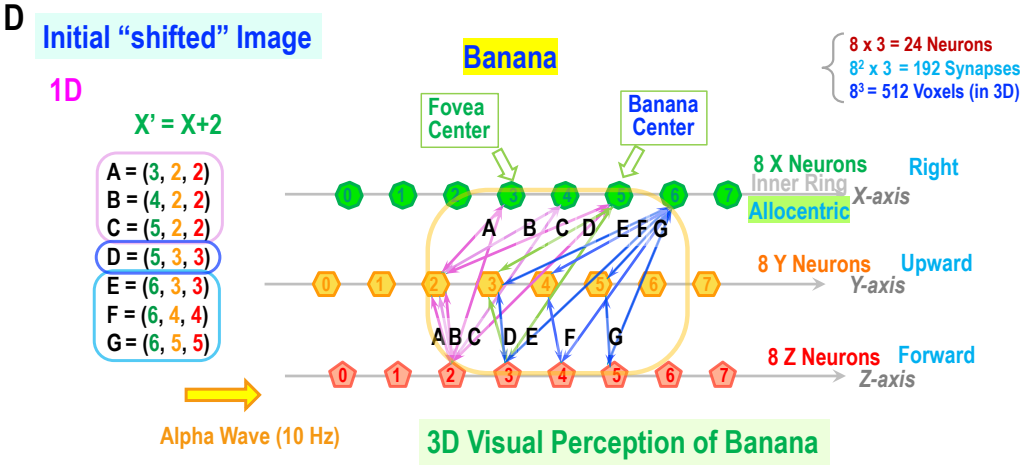
Initial "shifted" Image
1D
X' = X+2
A = (3, 2, 2)
B = (4, 2, 2)
C = (5, 2, 2)
D = (5, 3, 3)
E = (6, 3, 3)
F = (6, 4, 4)
G = (6, 5, 5)
Alpha Wave (10 Hz)
Banana
Fovea Center
Banana Center
8 x 3 = 24 Neurons
8² x 3 = 192 Synapses
8³ = 512 Voxels (in 3D)
8 X Neurons
Right
Inner Ring
Allocentric
X-axis
8 Y Neurons
Upward
Y-axis
8 Z Neurons
Forward
Z-axis
3D Visual Perception of Banana

E

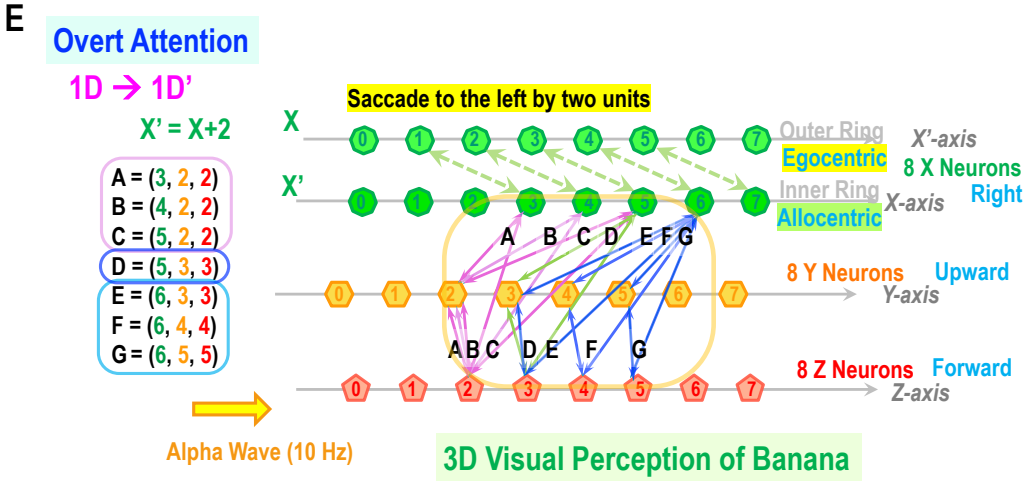
Overt Attention
1D → 1D'
X' = X+2
A = (3, 2, 2)
B = (4, 2, 2)
C = (5, 2, 2)
D = (5, 3, 3)
E = (6, 3, 3)
F = (6, 4, 4)
G = (6, 5, 5)
Alpha Wave (10 Hz)
Saccade to the left by two units
X
X'
Outer Ring
Egocentric
X'-axis
8 X Neurons
Right
Inner Ring
Allocentric
X-axis
8 Y Neurons
Upward
Y-axis
8 Z Neurons
Forward
Z-axis
3D Visual Perception of Banana

F

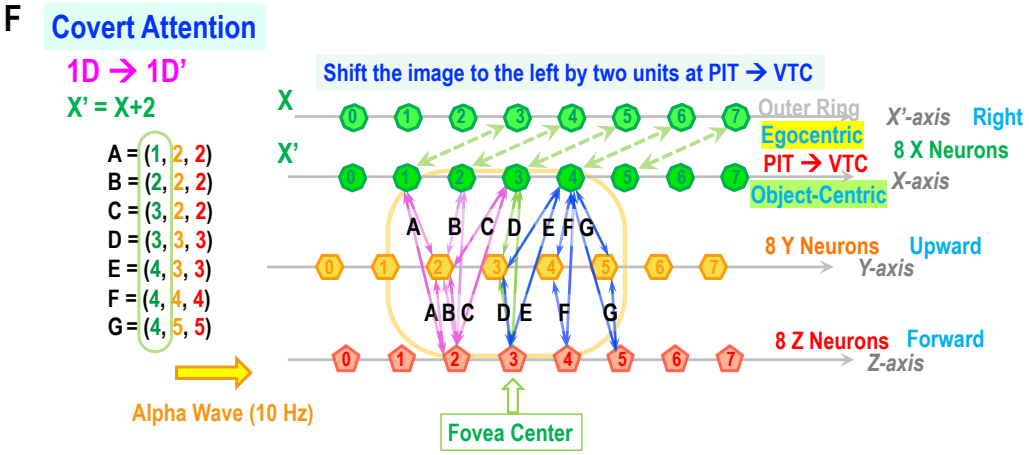
Covert Attention
1D → 1D'
X' = X+2
A = (1, 2, 2)
B = (2, 2, 2)
C = (3, 2, 2)
D = (3, 3, 3)
E = (4, 3, 3)
F = (4, 4, 4)
G = (4, 5, 5)
Alpha Wave (10 Hz)
Shift the image to the left by two units at PIT → VTC
X
X'
Outer Ring
Egocentric
X'-axis
Right
PIT → VTC
8 X Neurons
Object-Centric
X-axis
8 Y Neurons
Upward
Y-axis
8 Z Neurons
Forward
Z-axis
Fovea Center

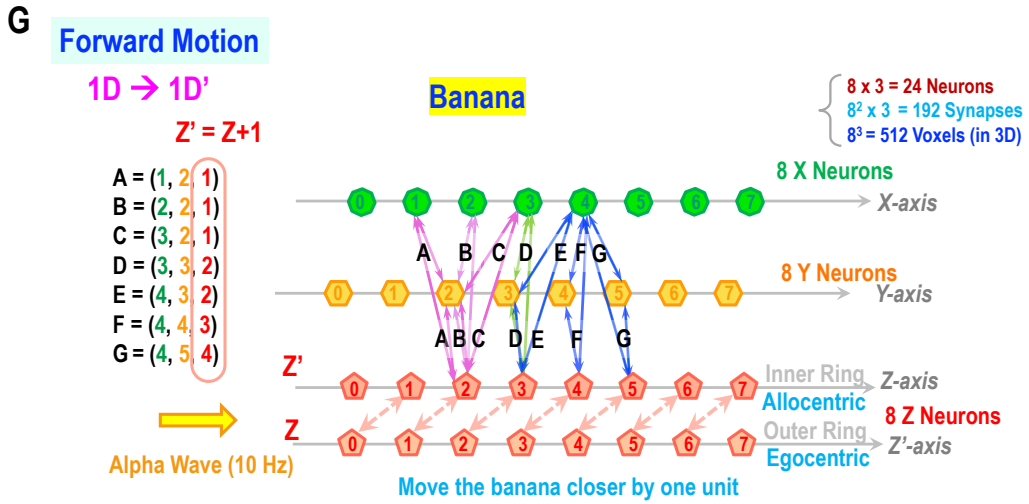

Figure 10. The holographic origin of overt and covert attention. **(A)** and **(B)** are the memorized 3D shape of a banana. **(C)** and **(D)** show a new retinotopic image of the same banana that is slightly shifted horizontally to the right by two pixels. **(E)** illustrates how overt attention works to recognize the banana shape while maintaining unchanged the allocentric frame. **(F)** illustrates how overt attention works to extract the semantic banana shape without a saccade. **(G)** shows the case when a host animal moves forward by one unit while maintaining unchanged the allocentric frame.

Please note that this mechanism of overt attention is identical to the insect's navigation system utilizing the ring attractor (**Section 1-2**); An insect reorients its body to the direction of food by the egocentric vision that is registered by the outer ring while maintaining the allocentric frame by the inner ring. Therefore, we could consider that our overt attention in vision is a natural evolutionary progression from the insects-like navigation system. And if horizontal overt attention corresponds to horizontal navigation of insects, our vertical overt attention must have originated from vertical navigation of the common ancestor of arthropods (e.g., insects) and vertebrates. This is the compelling reasoning behind our 3D navigation model for insects in **Figure 1**.

A similarity between our stable vision and rodents' navigation is equally remarkable. An observed landmark in the initial vision acts as a "place cell" in navigation. The place cell in navigation is anchored to the allocentric frame. Likewise, the initial landmark location in vision (like the center of the a banana) is anchored to the allocentric frame. That is why we observe external space consciously under the stable allocentric 3D space in vision.

Fundamentally, 3D vision and 3D navigation share the same coordinate system of [yaw, pitch, distance]. Thus, these two cases must share similar neural signal pathways and processing mechanisms. Furthermore, this principle should be universal from insects, to rodents, to humans. These two points are the essential outcomes of the **Grand Unified Theory of Mind and Brain**.

What about covert attention? This case is quite the opposite of overt attention; the observed image stays the same on a retina, before and after the covert attention shift. But through the ventral visual pathway, the egocentric image must be remapped onto the "object-centric" coordinate system, which is the coordinate system for the initial memory in **Figures 10-A** and **B**. This remapping must be coordinated holographically by an alpha phase shift, illustrated in **Figure 10-F**.

In real life, we usually perform covert attention first, followed by overt attention next. Through this two-step process, we can extract and recognize semantic 3D shape (like a banana) while maintaining an unchanged allocentric frame. These two distinct functions are the primary reason why our visual signal processing relies on two separate pathways: the ventral pathway for recognizing semantic shape and the dorsal pathway for maintaining the 3D allocentric frame. The entire process along the dual pathways is orchestrated by the PN to distribute proper phase shifts of alpha brainwaves. We will revisit this mechanism in detail in **Part III**.

Lastly, let us consider the case when we move forward (= Z direction) toward the banana (to pick up and eat it.) Since we consider visual perception in 3D, this situation is identical to overt attention as shown in **Figure 10-G**. This time, the allocentric frame is maintained by the alpha phase shift from Z (egocentric) → Z' = Z+1 (allocentric), very much like the maintenance of the place cell in the allocentric frame by theta phase precession.

This unification of navigation and vision in 3D is a remarkable outcome of the **Grant Unified Theory** that comprises **MePMoS** and **NHT**. Necessary conversion between the egocentric and allocentric frames is so smooth and prompt because the phase shifts in brainwaves conduct it. Without this new concept, it seems impossible to explain animals' extraordinary ability to internalize and maintain allocentric 3D space so stably.

Evolutionarily, one could imagine the following three steps: The first step was physical body motion towards food locations, which consumes lots of energy. The second step was overt attention, where we only move the eyes, which consumes subtle energy. And the third and last step was covert attention which takes almost no energy. We apply them from the opposite order in our daily activities: covert, overt, and finally, physical body motion. After all, evolution is a series of developments to maximize the amount of food while minimizing energy consumption.

3.4 Summary – Power of Holographic Tomography (NHT)

In summary, based on 2D and 3D toy models, we demonstrated how space could be expressed by the phases of brainwaves for visual perception and navigation. Furthermore, we showed how static memories can be formed naturally through Hebbian plasticity, leading to the concept of the "e*ngram*".

The consequence is significant; On one side, long-term static memory of 3D space is formed and stored by the 2D matrix of synapses under the allocentric frame. On the other side, sensory input is injected into the retinotopic 2D matrix of neurons under the egocentric frame. To link and compare the memories and senses, these two distinct types of the 2D matrices are converted into the frequency-time domain by **Neural Holographic Tomography (NHT)**, resulting in conscious perception in the case of 3D vision. Here, thanks to the prompt phase shifts orchestrated by the PN based on the corollary discharge, the allocentric frame of memory and the egocentric frame of sensation can meet in time coincidence, which satisfies Hebbian plasticity. Thus, causality and locality are satisfied, and **MePMoS** is realized.

These toy models in this **Section 3** show the essence of this paper; vision and navigation are truly unified in 3D by the shared coordinate system, the same holographic expression, and the same synaptic memory structure. And all animals from insects to humans share this unifying principle – that is the **Grand Unification of Mind and Brain**.
In the later **Section 5**, we will further develop the exact realization of **NHT** by a specific memory unit named **Holographic Ring Attractor Lattice (HAL)**. But before we move onto the concept of **HAL**, we shall define the required various coordinate systems in neural networks in the following **Section 4**.

4 3D Polar and Cartesian Coordinate Systems

4.1 Coordinate Systems to Describe Space in Human Brain

Function	Location in Brain	2D / 3D	Coodinate	Brain-wave	Center	Direc-tion	Axes of HAL	Scale
Vision								
2D Image	Eyes	2D	2D Linear	Retino-topy	Eye		[Yaw, Pitch]	N/A
2D Receptive Field	Primary (LGN→V1/V4)		Log-Polar				[Roll, Log(Ecc.)]	Log(Ecc.)
3D Space Construction	Dorsal (MT→FEF)	2D →3D	Linear-Polar				[Roll, Ecc., Log(Dist.)]	Log(Dist.)
3D Shape Recognition	Ventral (PIT→VTC)		Log-Polar	Alpha	Object		[Roll, Log(Ecc.), Log(Dist.)]	
Conscious 3D Vision	7a → Parahippo-campal Cortex	3D	Linear-Polar		Body		[Yaw, Pitch, Roll, Dist.]	Distance
Conscious 3D Space			Cartesian		Alloc.		[X, Y, Z]	N/A
Navigation								
Head Direction	(Everywhere)	3D	Linear-Polar	Beta	Head	Alloc.	[Yaw, Pitch, Roll, Speed]	Speed
Path Integration - In	Parahippocampal Cortex				Object		[Yaw, Pitch, Roll, Dist.]	Distance
			Cartesian	Theta	Alloc.		[X, Y, Z]	N/A
Map-based Navigation	EC-Hippocampus						[X', Y', Z', T] Hex tilted	N/A
Path Integration - Out	Retrosplenial Cortex		Log-Polar	Beta	Object		[Yaw, Pitch, Roll, Log(Dist.)]	Log(Dist.)

Table 1. A complete list of the existing coordinate systems in the human brain. From the top row to the bottom, this table follows the top-down signal processing by **MePMoS**, which is discussed in **Part I: Section 5.2-3** and illustrated in **Figures 13** and **14**.

To some extent, a brain is a well-designed machine for the frame conversion to internalize the external world. Throughout the discussion on navigation and vision, it has become clear that the precise definitions of various coordinate systems (frames) are essential. This **Section 4** is devoted to defining the coordinate systems in our brains, necessary for further investigation of the exact neural networks for navigation and vision. **Table 1** summarizes all the existing coordinate systems in the human brain for both 3D navigation and 3D vision. We shall go through the table, step by step.

The most crucial distinction is between the allocentric and egocentric coordinate systems. Obviously, the allocentric frame is assigned to absolute external space, independent of and unchanged by the location and direction of a host animal in that space. But specific attention is required to differentiate between the map center of the coordinate system and the direction (orientation) of the system. Naively speaking, the allocentric frame implicitly means that both the map center and the absolute direction (such as North) are allocentric. This is the case of map-based navigation given by place and grid cells. It follows our convention of regular maps, either printed or GPS-based ones.

On the other hand, path-integration-based navigation needs special attention. Path integration maintains the allocentric direction (like the North), but it does not keep the allocentric map center. The center of the coordinate is egocentric, either “head/body-centric” attached to the host animal’s head location or “object-centric” attached to landmarks.

Likewise, as for vision, one must consider specific distinctions for the egocentric frame attached to a host animal. To be exact, egocentricity can be applied independently to eyes, head, and body. To distinguish these three, we shall name them the "eye-centric," "head-centric," and "body-centric" frames. Our retinotopic image is "eye-centric," but conscious visual perception is "body-centric" because saccadic eye movements and head reorientation are compensated and unnoticed during conscious visual perception. In the case of covert attention, the concept of the egocentric frame must be applied to landmarks for the recognition and memory of semantic shapes along the ventral pathway towards VTC; it will be the "Object-centric" frame.

Then the second critical distinction is the Cartesian vs. polar coordinate system. The Cartesian is most widely used in regular mathematics and physics because of its simplicity, for 3D linear frame translation and summing up multiple vectors by individual components (x, y, z). On the other hand, the polar coordinate system fundamentally describes egocentric navigation and vision. The 3D polar coordinate is most often used for nautical and aerial navigation by [yaw, pitch, roll] angles. The navigation principle based on the polar coordinate system is named "*path integration*." The polar coordinate also gives our 2D vision by [yaw, pitch], ignoring the depth perception.

Lastly, the coordinate system could express distance by either linear or log scales. The Cartesian is normally a linear scale, whereas the polar coordinate can be either linear or log scale. The log-polar coordinate system is extremely important for scale invariance to extract semantic shape information by scaling up/down. The log-polar system is a unique feature of human's primary visual cortex system (Horton and Hoyt 1991; Benson et al. 2014; Abdollahi et al. 2014), while all other animals seem to have the simpler linear coordinate in their visual system (Garrett et al. 2014). We shall address it extensively in **Part III**.

4.2 Coordinate Systems in 3D Vision and 3D Navigation

Following the definitions and distinctions of various coordinate systems, **Table 1** summarizes all the existing coordinate systems in the human brain. From the top row to the bottom, this table follows the top-down signal processing by **MePMoS**, which is discussed in **Part I: Section 5.2-3** and illustrated in **Figures 13** and **14**. The top is 3D navigation based on the Hippocampal network that generates episodic memory, whereas the bottom is visual stimulation on the retina. The top is 3D Cartesian with the allocentric frame, whereas the bottom is the polar coordinate with the egocentric (eye-centric) frame. In between, our brain has several stages for holographic frame conversion.

3D human navigation relies on the both map-based frame by the Cartesian system (Moser, Kropff, and Moser 2008) and path integration by the polar coordinate system (Etienne & Jeffery, 2004) Map-based navigation is known to be coordinated by theta brainwaves as evidenced by rodents' place cells, grid cells, and theta phase precession (O'Keefe 1976; Moser, Kropff, and Moser 2008). On the other hand, path integration is strictly related to head/body direction vectors. We assume it is controlled by beta brainwaves ($f \sim 20$ Hz). More detail will be given in **Part IV**.

In this table from left to right, various coordinate systems are categorized in the columns below:

1) 3D Navigation (Map vs. Path integration) vs. 3D Vision
2) Cartesian vs. Polar coordinate systems
3) Linear coordinate by (X, Y, Z) vs. Polar coordinate system by [yaw, pitch, roll]
    a. Within the Polar coordinate: Linear-polar vs. Log-polar
4) Brain location that is responsible for expressing the holographic coordinates.
5) Type of brainwave: Theta (~5 Hz), Alpha (~10 Hz), and Beta (~20 Hz)
6) 3D map center and 3D direction: Allocentric vs. Egocentric
    a. Within Egocentric: Object-centric, Eye-centric, Head-centric, and Body-centric)
7) 1D scale factor: distance, Log(distance), Log(eccentricity), and Speed.

One striking fact is that 3D vision is based on the polar coordinate system of [yaw, pitch, roll], which is nearly identical to 3D navigation by path integration. In both polar coordinate systems of vision and navigation, Linear-scale and Log-scale representations appear to co-exist, which is a unique feature that is only observed in the human brain.

From the bottom, the visual signal must go through several stages; After the ventral pathway, 3D semantic shape is constructed by the log-polar coordinate system at VTC. On the other hand, along the dorsal pathway from MT to FEF, 3D space is constructed by the linear polar coordinate system at 7a. To be exact, sensory stimulation goes up following this order while changing coordinate systems:

1) Eye-centric 2D Linear-polar [yaw, pitch] image on the retina
2) Eye-centric 2D Log-polar (roll, log(eccentricity)) vision (V1→ V4)
3) Eye-centric 3D Linear-polar vision (MT → FEF)
4) Body-centric 3D Linear-polar vision (7a, after saccade correction)
5) Allocentric 3D Linear-polar [yaw, pitch, distance] navigation = Path integration (in Parahippocampal Cortex)
6) Allocentric Cartesian (Hexagonal X, Y, Z) navigation = place/grid cells (in Entorhinal Cortex)

How these frame translations are conducted by the alpha brainwaves via the PN network. It will take one cycle (~100 ms) that is nested in the one theta cycle (~200 ms), as shown in **Part I: Figures 13** and **14**. Details of both dorsal and ventral pathways will be extensively described in **Part III**.

4.3 Evolution of Coordinate Systems in the Brain

We have been through the evolutionary development of brains from the simplest animals, such as Hydra and *C. elegans*, to the most complex one of humans. **Table 2** summarizes the evolution of the coordinate systems corresponding to the order of animals' evolution from the top to the bottom using modern taxa as comparative examples of stages of brain evolution.

As shown here, the neural networks of *C. elegans* and Hydra merged into the ring attractor of insects for both vision and navigation. Since that time, the concept of the ring attractor has been well conserved with modification in birds, rodents, and vertebrates including humans. (Medina 2010). In this table, expected coordinate systems are listed together, even if they have not been observed yet (marked "No" on the right-most column.) These are primarily 3D vision and 3D navigation because the current experimental studies have been severely limited in 2D. Nevertheless, as described earlier in **Sections 2** and **3**, the extension from 2D to 3D is natural and straightforward by applying the concept of **NHT**.

It is intriguing to observe that polar and Cartesian co-exist throughout evolution, both in vision and navigation. Why does nature have utilized both coordinates in parallel? It is probably because both have their own clear advantages and disadvantages. The Cartesian is more commonly used in mathematics due to the convenience of summing vectors by deconvoluting (x, y, z) components. On the other hand, the polar coordinate is more natural from the egocentric view to point out the direction of an external landmark. Clearly, both coordinate systems are evenly utilized by both navigation and vision systems.

From the physics point of view, it is worth pointing out that the fundamental interaction in nature seems to follow the polar coordinate systems. Perfect examples are Newton's gravity between masses and Coulomb's force between electric charges. These laws are based on two-point interactions under the polar coordinate system, not the Cartesian.

[*More details of the evolution of the visual systems will be given in* **Part III: Section 8.3**. *The evolution of the navigation systems will be covered in* **Part IV: Section 4.4**.]

Animal Kind	Navigation or Vision	Dimen-sion	Cartesian vs. Polar	Linear vs. Log	Axes	Remarks	Proved ?
Hydra, Jelly fish							
	Navigation	1D	Polar	Linear	[Yaw]	Difused Nerve Ring	Yes
C. elegans							
	Navigation	2D	Cartesian	Linear	[X, Y]	CPG based	Yes
Insect							
	Vision	2D	Polar	Linear	[Yaw, Pitch]	2D image on Retina	Yes
		3D	Polar	Linear	[Yaw, Pitch, Distance]	2D Ring Attractor	No
	Navigation	2D	Cartesian	Linear	[X', Y']	1D Ring, 45° tilted	Yes
		3D	Cartesian	Linear	[X', Y', Z]	2D Ring, 45° tilted	No
Bird							
	Vision	2D	Polar	Linear	[Yaw, Pitch]	2D image on Retina	Yes
		2D	Polar	Linear	[Yaw, Pitch]	Primary Visual Cortex	Yes
	Navigation	3D	Cartesian	Linear	[X', Y', Z] 45° tilted	MEC - Hippocampus	No
Rodent							
	Vision	2D	Polar	Linear	[Yaw, Pitch]	2D image on Retina	Yes
		2D	Polar	Linear	[Yaw, Pitch]	Primary Visual Cortex	Yes
	Navigation	2D	Cartesian	Linear	[X", Y"] Hex grid	MEC - Hippocampus	Yes
		3D	Cartesian	Linear	[X", Y", Z"] Hex tilted	MEC - Hippocampus	No
Human							
	Vision	2D	Polar	Linear	[Yaw, Pitch]	2D image on Retina	Yes
		2D	Polar	Log	[Roll, Log(Eccentricity)]	Primary Visual Cortex	Yes
		2D	Polar	Linear	[Roll, Eccentricity]	Dorsal (MT-FEF)	No
			Polar	Linear	[Yaw, Pitch, Roll, Distance]	Dorsal (FEF-7a)	Yes
		3D	Polar	Log	[Yaw, Pitch, Roll, Log(Dis.)]	Ventral (VTC)	No
	Navigation	2D	Cartesian	Linear	[X", Y"] Hex grid	Entorhinal Cortex	Yes
		3D	Cartesian	Linear	[X", Y", Z"] Hex tilted	Entorhinal Cortex	No
		3D	Polar	Linear	[Yaw, Pitch, Roll, Distance]	Parahippocampal Cortex	No
		3D	Polar	Log	[Yaw, Pitch, Roll, Log(Dis.)]	Retrosplenial Cortex	No

Table 2. Summary table of coordinate systems of various animals. From top to bottom, it follows evolutionary developmental stages.

From the most fundamental point of view in physics, the Universe consists of elementary particles such as electrons and quarks with specific masses and charges. In a way, landmarks for animals are like these particles in physics. Considering this analogy, it appears natural for brains to apply the polar coordinate system (= the same coordinate as particle interactions) to identify landmarks and act on them. We will revisit this analogy between particle physics and neurophysics in **Part VI**.

In this section, we have spelled out all the necessary coordinate systems. By utilizing these systems, the following **Section 5** will establish the exact structure of synaptic memories, the *engram*, named the **Holographic Ring Attractor Lattice (HAL).**

5 Holographic Ring Attractor Lattice (HAL) for 3D Polar Coordinates

5.1 Holographic Ring Attractor Lattice (HAL) as an Engram

In the previous **Sections 2** and **3**, using a few toy models, we introduced the new concept of **Neural Holographic Tomography (NHT)** that has defined a new concept of static synaptic memory for 2D and 3D navigation and vision. This **Section 5** will modify these toy models to represent more realistic mechanisms of 3D perception and memory by employing the exact coordinate systems defined in **Section 4**.

To begin with, we will introduce a promising accurate neural network structure, a realistic candidate of the e*ngram*, in the following four steps, shown in **Figure 11**.

1) We first start from **Figure 11-A,** which is identical to **Figure 5-C** for 3D navigation and to **Figure 9-C** for 3D vision. We keep three strings(rows) of 8 neurons (from No. 0 to No. 7). The only modification in **Figure 11-A** is that after Neuron No. 7 on the right, the brainwave should return to the left to repeat the traveling wave again. This link from Neuron No. 7 to No. 0 allows forming a ring attractor. Here, we also assume that the phase is zero and the spike rate is highest at Neuron No. 0 on the left.
2) Secondly, as shown in **Figure 11-B,** we double the total number of neurons per line from 8 to 16. The center point (= Neuron No. 0) corresponds to phase zero. Then, after a half period to the right, the wave returns to the left and keeps running to complete the second half.
3) Thirdly, in the same **Figure 11-B**, the fourth axis is added corresponding to time cells, with which a complete 4D space-time can be presented.
4) Fourthly, in **Figure 11-C,** the total number of strings (= rows) is doubled from 4 to 8. The brainwaves on the odd-number strings travel to the right, whereas the even-number strings carry the brainwaves to the left. On each line, after 8 neurons on the right (or left) side from the center, a brainwave reaches a half period (phase = $\pm\pi$.) and then returns to the opposite side, keeping a continuous cycle. Thus, the eight strings of 16 neurons behave as eight ring attractors. [*By doing so, the opposite direction of waves on the adjacent even and odd strings collide with each other, producing a standing wave, which is the origin of the grid cell as shown later in* ***Part IV***.]

We shall name this lattice structure in **Figure 11-C**, **Holographic Ring Attractor Lattice** (**HAL**).

[*HAL 9000 is the fictional Artificial Intelligence in the 1968 film, "2001: A Space Odyssey." HAL 9000 is capable of natural language processing, facial recognition, etc... We will address similar cognitive abilities in humans enabled by the* ***HAL*** *later in* ***Part VI***.]

The outcome is a compressed lattice array of 16 (neurons) x 4 (dimensions) x 2 (strings) = 128 neurons. Each neuron has two-way connections with all other neurons; thus, a total of 8 x 16 x 2 = 256 synaptic links are formed at each neuron (which is realistic since a single neuron is known to have typically ~1,000 synapses on average.) Thus, a single **HAL** comprises 128 x 256 = 32,768 synapses. Effectively, various possible synaptic linkages correspond to all possible points in 4D space-time consisting of $16^4 \approx$ 66k voxels in 4D.

HAL can be considered as a universal memory unit, that is, an *engram*. Nevertheless, it should be noted that the proposed **HAL** above is a hypothetical lattice structure, yet to be discovered and verified experimentally. Therefore, the exact proposed configuration may still have some ambiguity and loose ends to be determined.

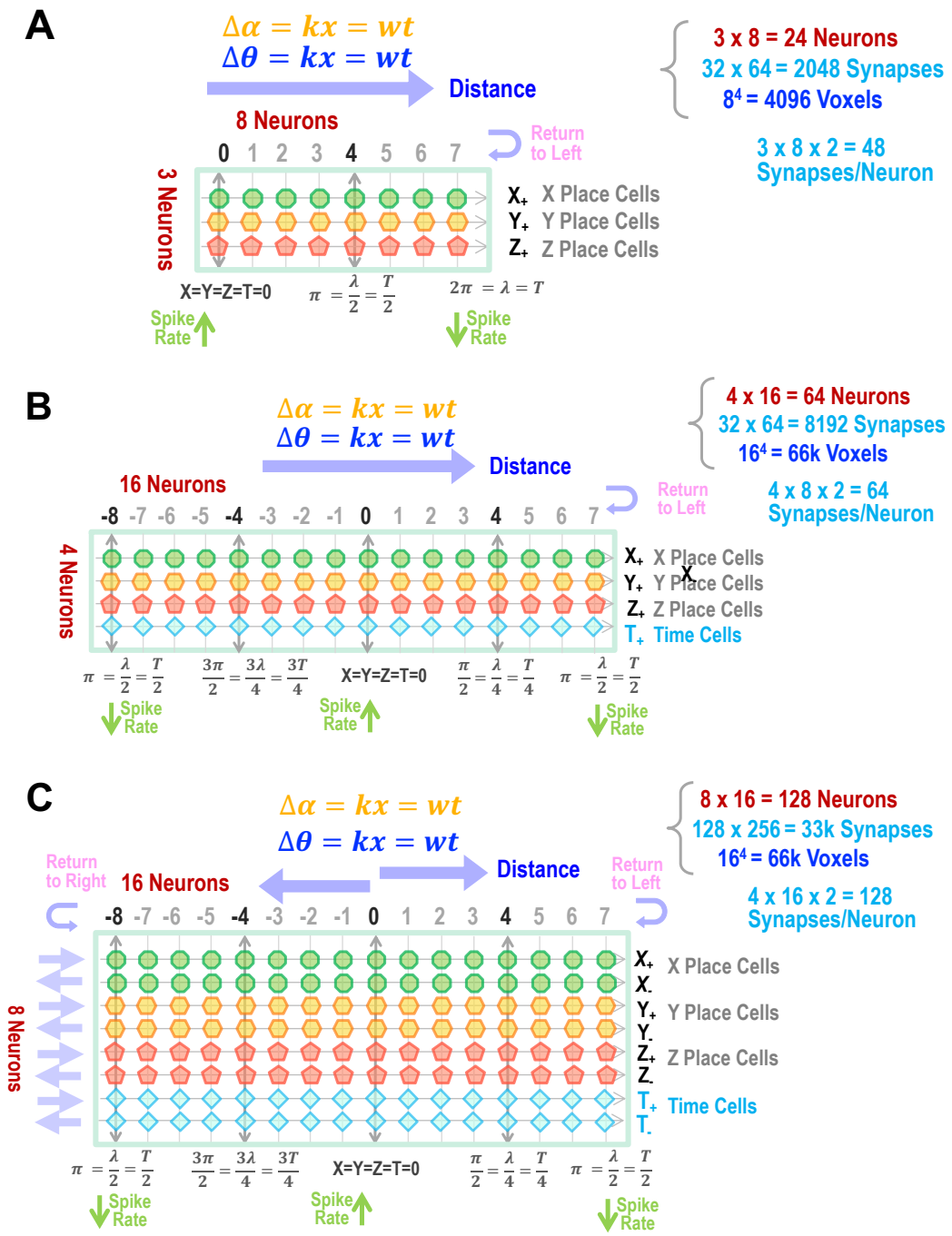

Figure 11. **Holographic Ring Attractor Lattice** (**HAL**). **(A)** is the simplest **HAL** that is identical to **Figure 5-C** for 3D navigation and to **Figure 9-C** for 3D vision. The only difference is that after Neuron No. 7, the brainwave returns to the left to repeat the traveling wave again, forming a ring attractor. We also assume that the phase is zero and the spike rate is the highest at Neuron No. 0. **(B)** is extended from (A) from 8 horizontal neurons to 16 neurons. After a half period, the wave returns to the left to complete the second half. The fourth axis, the time axis for time cells, is added to represent 4D space-time**.** **(C)** is the final proposed **HAL**, which includes the positive and negative directions of waves, resulting in a total of 8 strings of 16 neurons.

In previous **Sections 2** and **3**, we already introduced the following three types of brainwaves to the space-time diagram of the human brain. They are all supposed to form the **HAL**.

1) Theta brainwaves (~5 Hz) enable GPS-like 3D navigation by the Cartesian coordinate system.
2) Alpha brainwaves (~10 Hz) facilitate the visual perception of the 3D allocentric frame
3) Beta brainwaves (~20 Hz) provide 3D head direction vectors for navigation based on path integration.

Here in the remaining section, we will comprehensively explore these functions of **HAL**. Later in **Parts III** and **IV**, we will further apply **HAL** to human 3D vision and navigation in extreme detail. Then in **Part V**, all five senses (vision, hearing, touch, smell, taste) will be described universally by the **HAL** altogether, which will exhibit the full power of the **Grand Unified Theory**.

5.2 An Example of HAL for 3D Direction Vector – Head Direction Cells

One of the primary navigation strategies is by path integration (Etienne & Jeffery, 2004), which is based on the direction vector in the polar coordinate system. Here, let us apply the concept of **NHT** and **HAL** to precisely describe the process of path integration in 3D. As shown in **Figure 11**, we follow the established concept of the insect's ring attractor for 2D navigation (**Section 1.2**) and extend it to 3D. **Figure 12-A** defines generalized rotations in 3D by the polar coordinate system with [yaw, pitch, roll] angles, where yaw corresponds to azimuth and pitch corresponds to altitude (i.e., elevation).

We then consider the ring attractors shown in **Figure 12-B**, where the three rotations in [yaw, pitch, roll] are scanned by a total of the six beta brainwaves (f ~20 Hz) by running in both clockwise and counterclockwise directions. Furthermore, we assume 16 neurons (= segments) per circle (= period). (Please note that the insect's ring attractor has only eight neurons per left/right direction. Therefore, we are doubling the segments.) In addition to 3 x 2 = 6 rotations, we will include the fourth dual-ring structure to store speed (instead of the time axis in **Figure 11-C**), resulting in 4 (degrees of freedom) x 2 (directions of brainwaves) = 8 rings of attractors. The name of "ring" attractors is perfect in this case because these rings literally represent three circles of [yaw, pitch, roll] in the polar coordinate system as presented in **Figure 12-B**.

In the case of animals more advanced than insects, these eight rings can be compressed into a flat lattice structure at their next evolutionary stage, by splitting between the -8^{th} and $+7^{th}$ neurons as shown in **Figure 12-C**. Please note that the physical ring shape in **Figure 12-B** and the lattice structure in **Figure 12-C** are topologically identical with the same synaptic connections; at the right end of the lattice, after the $+7^{th}$ neurons, synaptic connections go back to the left end to the -7^{th} neurons.

One should note that, in **Figure 12-C**, the horizontal axis corresponds to the direction of the traveling beta brainwaves (f ~20 Hz, T ~50 ms), to the right (on odd rows), and to the left (on even rows). As a result, each horizontal neuron has a specifically assigned phase of the beta brainwave, equivalent to a timestamp with (~50 ms) /16 = ~3 ms resolution. Such a time resolution is consistent with the narrow time window of Hebbian plasticity.

This concept and the structure, named **HAL,** will repeatedly appear throughout the remaining sections as the universal memory unit, which is a possible candidate of the *engram*, reviewed by (Schacter, Eich, & Tulving 1978; Josselyn 2010; Josselyn & Tonegawa 2020; Eichenbaum 2016).

In the case of **Figure 11-C** and **Figure 12-C**, consisting of 8 horizontal strings with 16 neuron segments each, a **HAL** contains a total of 8 x 16 = 128 neurons. Each neuron has two-way connections with all other neurons; thus, a total of 8 x 16 x 2 = 256 synaptic links are formed at each neuron. It means a single **HAL** comprises 128 x 256 = 32,768 synapses. Effectively, various possible synaptic linkages correspond to all possible direction vectors in 3D space consisting of $16^4 \approx 66$k directional voxels (i.e., directional vectors).

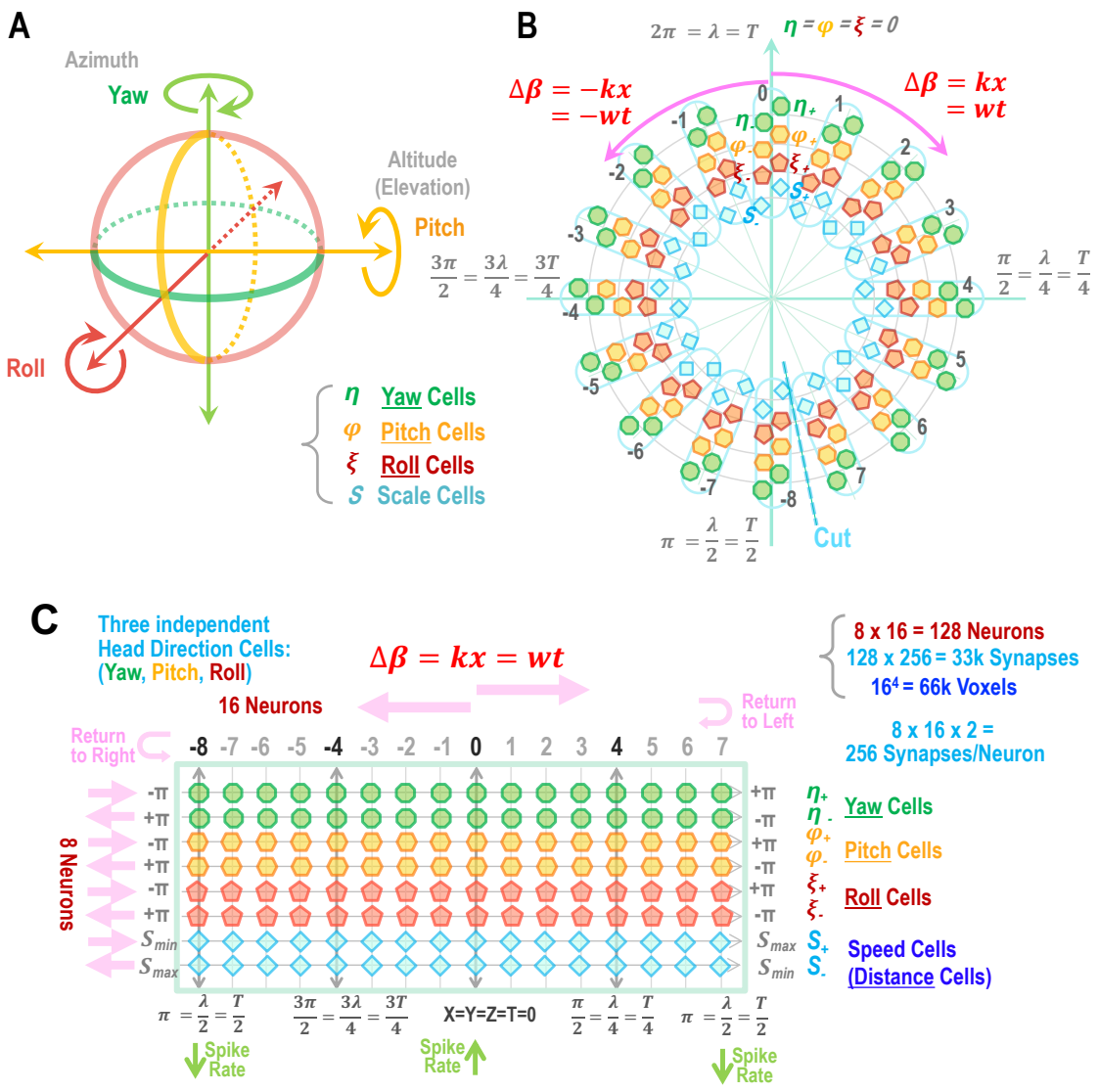

Figure 12. 3D Direction HAL by beta brainwaves. **(A)** defines the 3D rotation in [yaw, pitch, roll]. **(B)** shows the 3D Ring Attractor. Three rotations of [yaw, pitch, roll] are scanned by a total of the six beta brainwaves, running at both clockwise and anti-clockwise directions. **(C)** is the **Holographic Ring Attractor Lattice (HAL)**. With 8 horizontal strings with 16 neuron segments each, a **HAL** contains a total of 8 x 16 = 128 neurons. Each neuron is mutually connected with all other neurons in dual ways.

The proposed **3D Direction HAL** structure with traveling brainwaves enables the recording of multiple 3D direction vectors from a landmark to many other landmarks in parallel. Let us consider a navigation process like the one demonstrated in **Figure 1**, which consists of zigzag trajectories. The endpoint of the direction vector can be recorded in a **HAL** at the end of each segment of the trip, which creates a possibility for recording the locations of multiple landmarks in one trip. This is the principle of path integration, which brings about a significant evolutionary advantage over the insect ring attractor.

Please note that, in the case of insects, direction vectors are encoded by spike rates. However, in the case of **HAL**, direction vectors are encoded by phases of brainwaves, which are basically spike timings. Therefore, conversion from spike rates to spike timings must be adopted by **HAL**. Such conversion was observed, at least, in the case of the visual cortex V1 in cats (Gray & Singer, 1989) and monkeys (Fries et al., 2007; Vinck et al., 2013), as mentioned earlier in **Section 2.3**. Or perhaps, both spike rates and brainwave phases (timings) may co-exist, as discussed later **in Section 7.1**.

It is also worth noting that, these neurons in **HAL** are the origin of the observed "head direction cells" (Taube, 2007) and "speed cells" in rodents (Kropff et al., 2015). To be exact, the reported head direction cells correspond to the head "yaw" cells in the **HAL**. On one hand, this **HAL** is effectively utilized to keep a record of the animal's own velocity unit vector in 3D; the proper phases of beta brainwaves in the three directions are updated in real time, after corollary discharges from each head or body movement are received and distributed via the pulvinar nuclei (PN). More details will be given in **Part IV** for the case of the rodent navigation system.

In addition, we could consider a similar but different type of **HAL**, which keeps track of the overall traveling direction and length by integrating velocity vectors in time (as an insect does). Instead of "speed cells", this type of **HAL** must have "distance cells." Therefore, to be exact, there are two kinds of **HALs** for 3D direction vectors: "**3D Velocity HAL"** (with speed cells) and "**3D Distance HAL"** (with distance cells). These two **HAL**s together offer the basis for the comprehensive description of the path-integration-based map for multiple landmarks, as shown later in **Part IV**.

5.3 3D Polar HAL for 3D Vision

As the second application of the **HAL**, let us consider our 3D visual perception, given in **Figure 13**. As we already discussed in **Section 3**, the basic principle of 3D vision by **NHT** is a natural extension of the 3D navigation system, thus both are remarkably similar. Especially, 3D navigation by path integration and 3D vision share the identical polar coordinate system given by the three orthogonal rotating angles of [yaw, pitch, roll] with distance as the fourth axis.

It is worth noting that navigation in 2D is given by the flat horizontal plane of [yaw, distance] whereas the 2D vision is based on the vertical plane of [yaw, pitch]. So, these two 2D spaces appear disconnected except the yaw angle (= azimuth). However, once 2D is extended to realistic 3D, navigation and vision share the identical 3D frame, expressed by the polar coordinate system given by the four degrees of freedom of [yaw, pitch, roll, distance]. This fact strongly indicates that both navigation and vision must be constructed in the same 3D frame and share the identical 3D representation, a key aspect of the **Grand Unified Theory**. From an evolutionary point of view, primitive animals must have navigated space blindly without vision. Therefore, one can speculate that the navigation system evolved from 2D to 3D first, and then next a 3D vision system was naturally invented as a spin-off of the 3D navigation system. In other words, vision must have been designed not for 2D but for 3D perception with depth perception from the beginning.

If so, what distinguishes 3D vision from 3D navigation in the brain? Essentially it is the frequency of the brainwaves. It is well-known that the alpha brainwave is related to vision, so we will assign alpha for 3D vision as shown in **Figure 13**, instead of the beta for 3D navigation by path integration in **Figure 12**. Otherwise, both **Figures 12** and **13** are identical. Here, we begin to see the effectiveness of the new concept of **HAL** as a candidate for an *engram*.

In the case of 3D vision in **Figure 13-C**, the horizontal axis is the direction of the traveling alpha brainwaves (f ~10 Hz, T ~100 ms) to the left and to the right. Thus, each horizontal neuron has a specifically assigned phase of the alpha wave, equivalent to a timestamp with (~100 ms) /16 = ~7 ms resolution. Such a time resolution is comfortably wider than a typical time window of Hebbian plasticity.

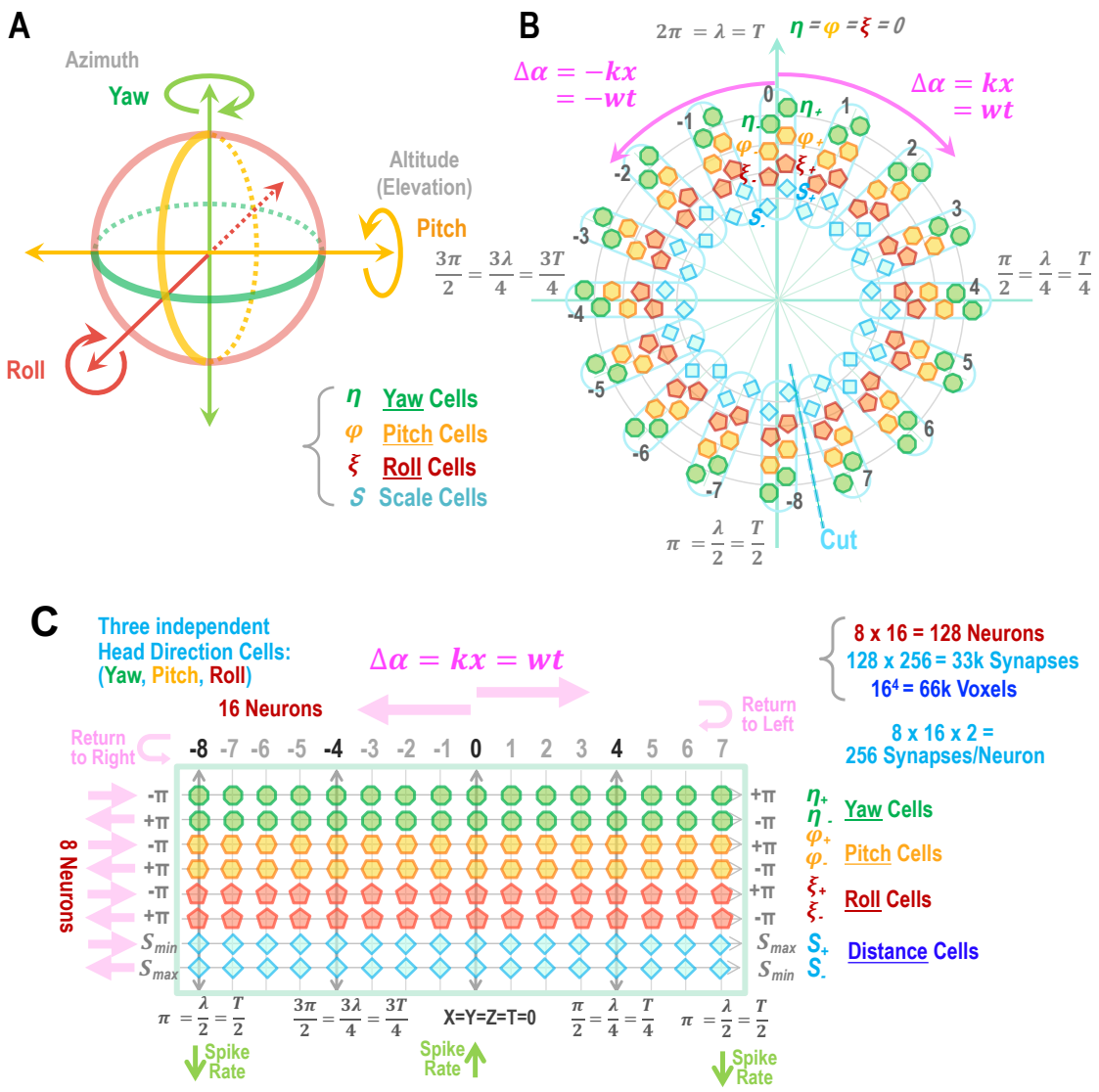

Figure 13. 3D Polar Vision HAL by alpha brainwaves, which is identical to **3D Direction HAL** in **Figure 11. (A**) defines the 3D rotation in [yaw, pitch, roll]. **(B)** shows the 3D Ring Attractor. Three rotations of [yaw, pitch, roll] are scanned by a total of six beta brainwaves, running at both clockwise and anti-clockwise directions. **(C)** is the **Holographic Ring Attractor Lattice (HAL)**. With 8 horizontal strings with 16 neuron segments each, a HAL contains a total of 8 x 16 = 128 neurons. Each neuron is mutually connected with all other neurons in dual ways.

On the other hand, one may wonder that our visual acuity is far superior to 16 pixels, like more than 1,000 pixels in horizontal and vertical directions. This is a critical valid concern, thus we will address this discrepancy later in **Section 7** and **Part III-IV**, by introducing the Discrete Fourier Transformation (DFT) and the bottom-up gamma band ($f > 40$ Hz) brainwaves.

In the human visual pathway, the primary visual cortex from V1 to V4 is known to exhibit 2D Log-polar coordinates given by [roll, log(eccentricity)] (Horton and Hoyt 1991; Benson et al. 2014; Abdollahi et al. 2014), which seems to carry over through the ventral pathway from PIT to VTC.

On the other hand, at the end of the dorsal pathway, after FEF to 7a, we consciously perceive 3D visual space by [yaw, pitch, distance]. **Part III** will go through the complete treatments of these specific coordinate systems.

5.4 Frequency/Phase Assignment by the PN Network

So far, we assumed that specific frequencies and phases are assigned to **HAL** a priori, like the beta wave (~20 Hz) for navigation by path integration, and the alpha wave for vision (~10 Hz). However, this is not necessarily the case, especially for phase assignments. As an *engram*, **HAL** is destined to memorize meaningful static information under the universal allocentric frame. On the other hand, sensory stimulation enters within the egocentric frame. This mismatch of allocentric and egocentric frames is where **NHT** plays the central role. As demonstrated by the toy model of 3D vision in **Section 3.3**, information can be transformed between the two coordinate systems through communication via time, or brainwave phase, holographically.

Fundamentally, this frame mismatch is caused by the host animal's constant motion, either of its eyes, head, or body. For every single movement, the egocentric frame must be reallocated within the allocentric frame in real-time. This so-called remapping is orchestrated by the Pulvinar Nuclei (PN) (Bridge et al. 2016)(Soares et al. 2017). As mentioned in **Part I: Section 5.5**, PN receives corollary discharges from motor neurons. It acts as the central clock that distributes the proper brainwaves with specific phase assignments to the entire cortex. Llinás demonstrated that the higher membrane potential of neurons in PN increases the frequency of brainwaves, whereas lower potential in PN neurons reduces the frequency (Llinas 2014). In the extreme case of the potential momentarily going below threshold, the brainwave would be shut off during that short period. Such a quick turn-off of the brainwave effectively increases the phase. The cortical-wide distribution of the exact frequencies and phases are regulated by gap junctions (Coulon & Landisman, 2017). [*Please note that this concept of PN-based phase shift is a new idea, yet to be tested experimentally in the future*.]

The above-mentioned real-time distribution of brainwaves with proper phases is the heart of executing **MePMoS** by the principle of **NHT**, utilizing **HAL**. This phase distribution from PN is illustrated in **Part I: Figure 14** between 100 – 200 ms by the pink arrows. Since the updated phases are dynamically assigned based on the host's motion, this process is essentially top-down. The allocentric frame will be maintained all the time in our conscious perception of 3D space, while unconscious egocentric retinotopy is properly transformed to the allocentric frame by shifts in the phase of the brainwave.

The neatest example would be the case of 3D visual perception. The chart below summarizes how the egocentric 2D retinotopy from the bottom communicates with allocentric 3D visual perception and memory at the top (in **Part I: Figure 14**.) Detailed analysis and description of these processes will be given in **Part III**.

	[Bottom]	"Invisible" 2D Egocentric Retinotopy	(32 x 32 = 1028 Neurons)
← →		"Visible" 3D Holographic Tomography (**NHT**)	(8x16 =128 Neurons, 16^4 = 66k Voxels)
← →	[Top]	"Invisible" 3D Allocentric Memory (**HAL**)	(128 x 256 = 33k Synapses)

6 3D/4D Linear HAL for 3D/4D Cartesian Space-time

6.1 Principle of 3D/4D Linear HAL – Place Cells and Time Cells

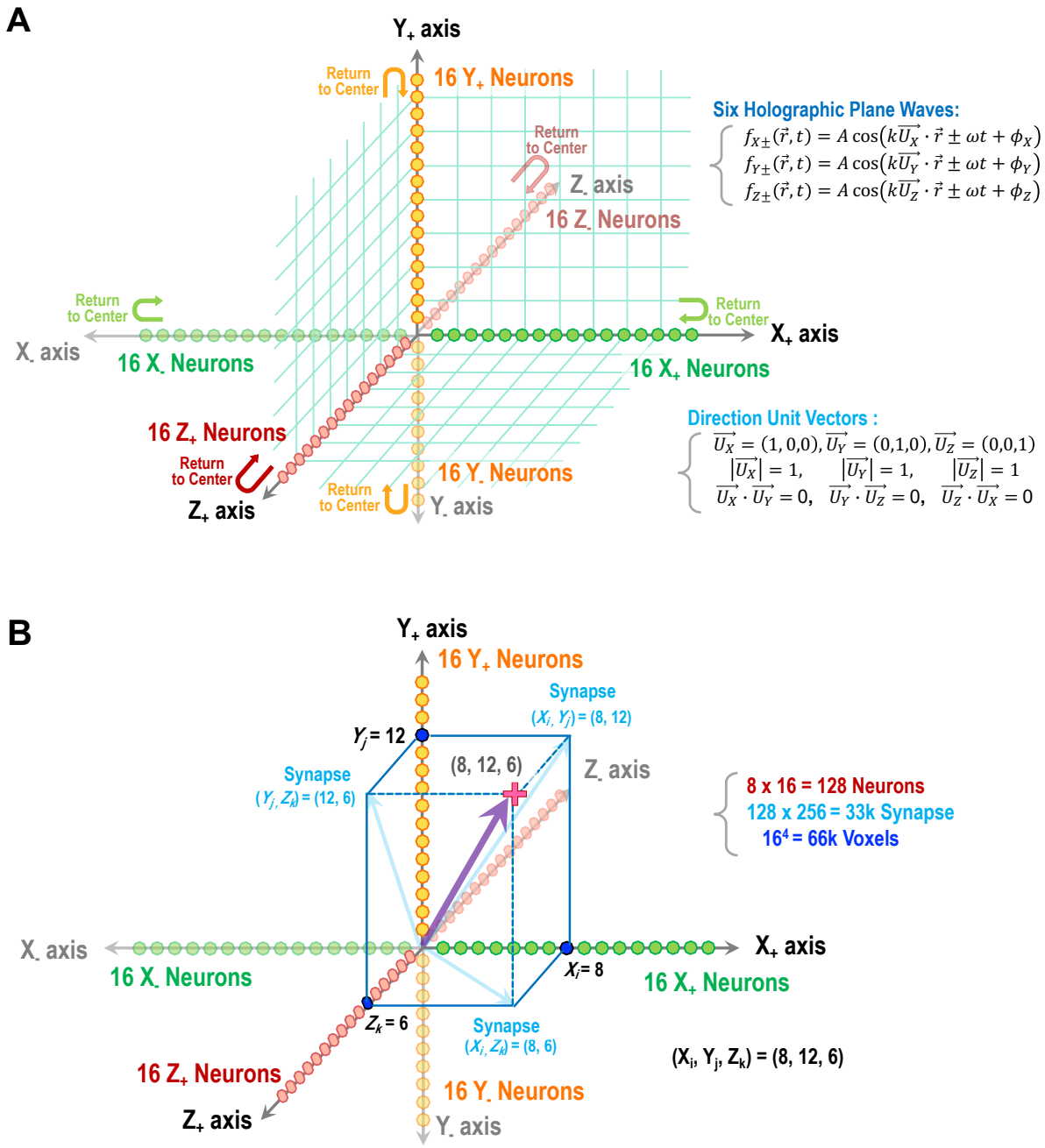

Figure 14. The formation of the **3D Space-time HAL** by six theta brainwaves. **(A)** Six holograpic brainwaves are traveling towards the six orthogonal directions. Then, after 16 linear neurons, the brainwaves return to the center of the coordinate system. **(B)** An example of a landmark at the position (X_i, Y_j, Z_k) = (8, 12, 6). This is the origin of place cells.

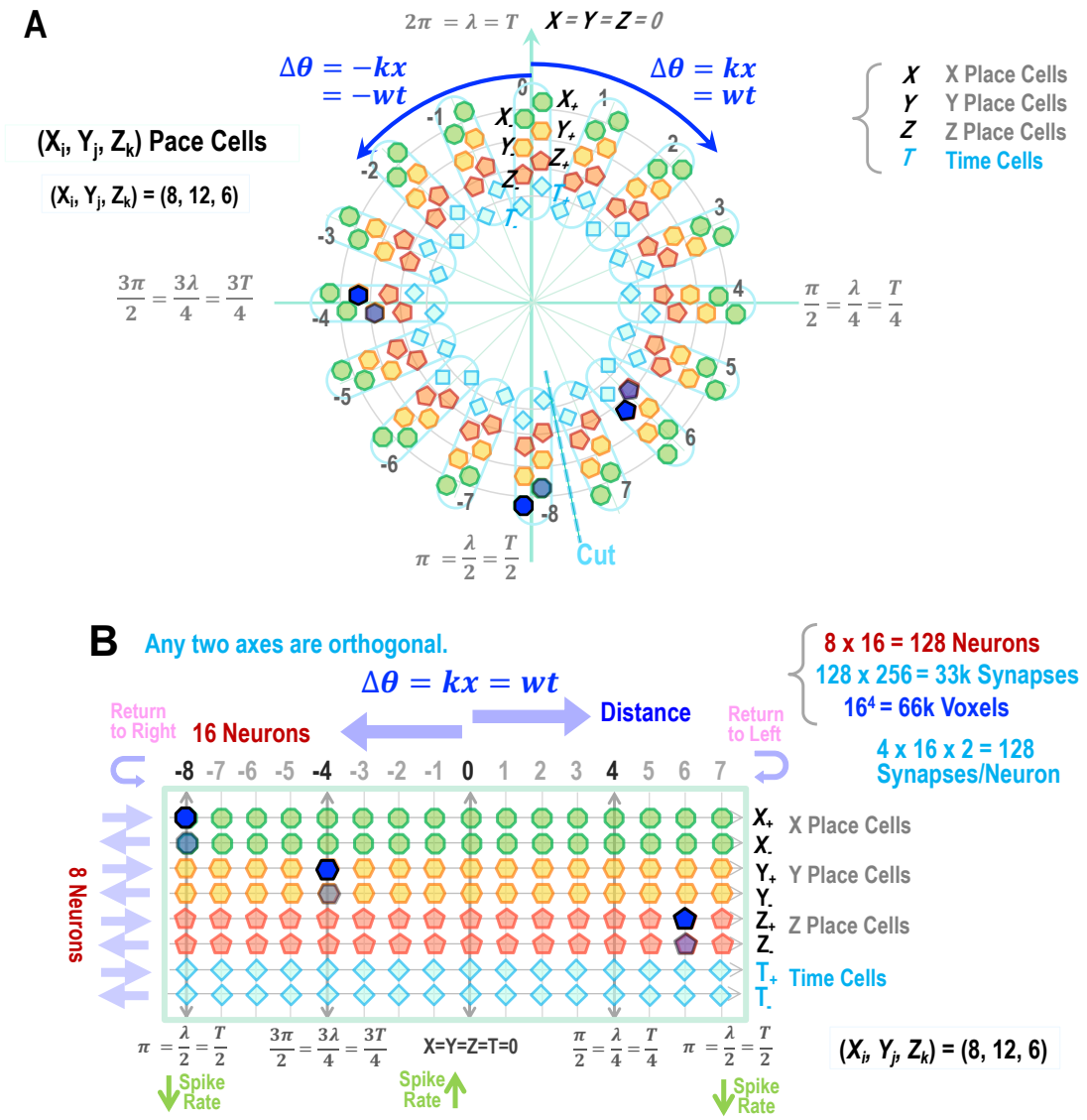

Figure 15. 4D Space-time HAL. **(A)** The ring attractors of the 4D Space-time HAL. **(B)** The actual lattice structure of the 4D Space-time HAL. The place cells, $(X_i, Y_j, Z_k) = (8, 12, 6) = (-8, -4, 6)$ are marked.

The other well-known, critical navigation principle is based on the 3D Cartesian coordinate system, like a Global Positioning System (GPS). Let us consider a standard orthogonal coordinate system of (x, y, z), shown in **Figure 14-A**. Listed on the right side are six sets of unit vectors and the theta brainwaves traveling in these directions. We take the notation of

x: horizontal (+/- = left/right), y: vertical (+/- = up/down), and z: depth (+/- = forward/backward).

For each one of the six directions, 16 linear neurons are assigned to form the 3D direction **HAL**. At the end of the 15th neurons, brainwaves return to the 0th neurons with zero phases at the center of the 3D Cartesian coordinate system. It is like a wheel traveling along the direction of each axis; after one rotation, the same point on the wheel touches the ground.

Figure 14-B shows an example of a landmark at $(X_i, Y_j, Z_k) = (8, 12, 6) = (-8, -4, 6)$. Here, (i, j, k) represents the integer number of the neurons at the location (X, Y, Z). Please note that n = 8, 9, 10, 11, 12, 13, 14, 15 are equivalent to n = -8, -7, -6, -5, -4, -3, -2, -1 respectively due to a period = 16 (corresponding the phase = 2π.)

Following the principle and the construction procedure of the **HAL** established above, we can realign these 16 linear neurons (multiplied by 6 directions) as a ring attractor as shown in **Figure 15-A**. In this case, the fourth dimension – the time-axis – can be included (instead of speed or distance, as in the 3D Direction HAL in **Figure 12**.) Please note that all (x, y, z, t) have both clockwise and counterclockwise directions, forming a total of eight nested rings. Here, the place cell, $(X_i, Y_j, Z_k) = (8, 12, 6)$, is marked by 3 x 2 = 6 neurons. (Time is not assigned.) Finally, this ring attractor can be compressed into a compact lattice structure by dividing the rings between the 15^{th} and 0^{th} neurons, as shown in **Figure 15-B**. The place cell, $(X_i, Y_j, Z_k) = (8, 12, 6)$, is marked here again.

These six neurons represent the location of the landmark in the 3D Cartesian coordinate system, forming the well-known "place cells" in 3D. When an animal arrives at that location, these neurons are synchronized by the theta brainwaves with zero phases and fire together. More detailed treatment is presented in **Part IV**. This **HAL** represents the 4D space-time by 8 strings x 16 linear neurons = 128 neurons. It means that, effectively, 4D space-time is converted to 1D (space) + 3D (time, or brainwave phase) by the **NHT**. This 4D expression also includes the observed time cells along the last two strings of neurons. 4D space-time is faithfully represented by the 2D matrix of synaptic connection of 128 x 128 x 2 ≈ 33k.

Figures 14 and **15** show the basic principle of holographic expression of 4D space-time. The exact applications will be given in the three cases below in respective sections:

1) Bird's navigation system: **Section 6.2**
2) Rodent's navigation system: **Section 6.3** and **Part IV**
3) Human's 3D visual perception: **Part III**

6.2 A Possible 3D/4D Linear HAL: from Insects to Birds

The 3D Cartesian coordinate system in **Figure 14** makes sense from the perspective of regular mathematics and physics. However, the evolution of animals might have taken a different orientation of three axes. Indeed, as introduced in **Section 1.2** in **Figure 1**, recent research has revealed that, in the case of insects, their 2D Cartesian coordinate system is formed by the two orthogonal axes tilted from the forward/ backward axis by 45 degrees (Lyu, Abbott, & Maimon, 2020). Therefore, if insects already developed holographic memories based on the **HAL**, they are likely to maintain these 45-degree-tilted axes, as shown in **Figure 16**.

We could further speculate that birds might utilize the same kind of tilted Cartesian coordinate system. In **Figure 16-A**, the directions of the three theta brainwaves are given with mathematical formulae. In **Figure 16-B**, two possible landmarks (= two types of flowers) are illustrated as two place cells. Please note that this figure is identical to Figures **4** and **5** in **Section 4.5,** where we introduced the toy model of 3D navigation, except both X and Y axes are 45 degrees tilted in **Figure 16,** and these neurons form the same **HAL** as shown in **Figure 15**.

6.3 3D/4D Linear HAL of Primates by the Tilted Hexagonal Geometry

Perhaps the most important interesting application of the **HAL** is for the 3D human navigation system. It must be similar to that of rodents because both share comparable hippocampal networks for navigation with observed place cells and grid cells (Moser, Kropff, & Moser 2008).

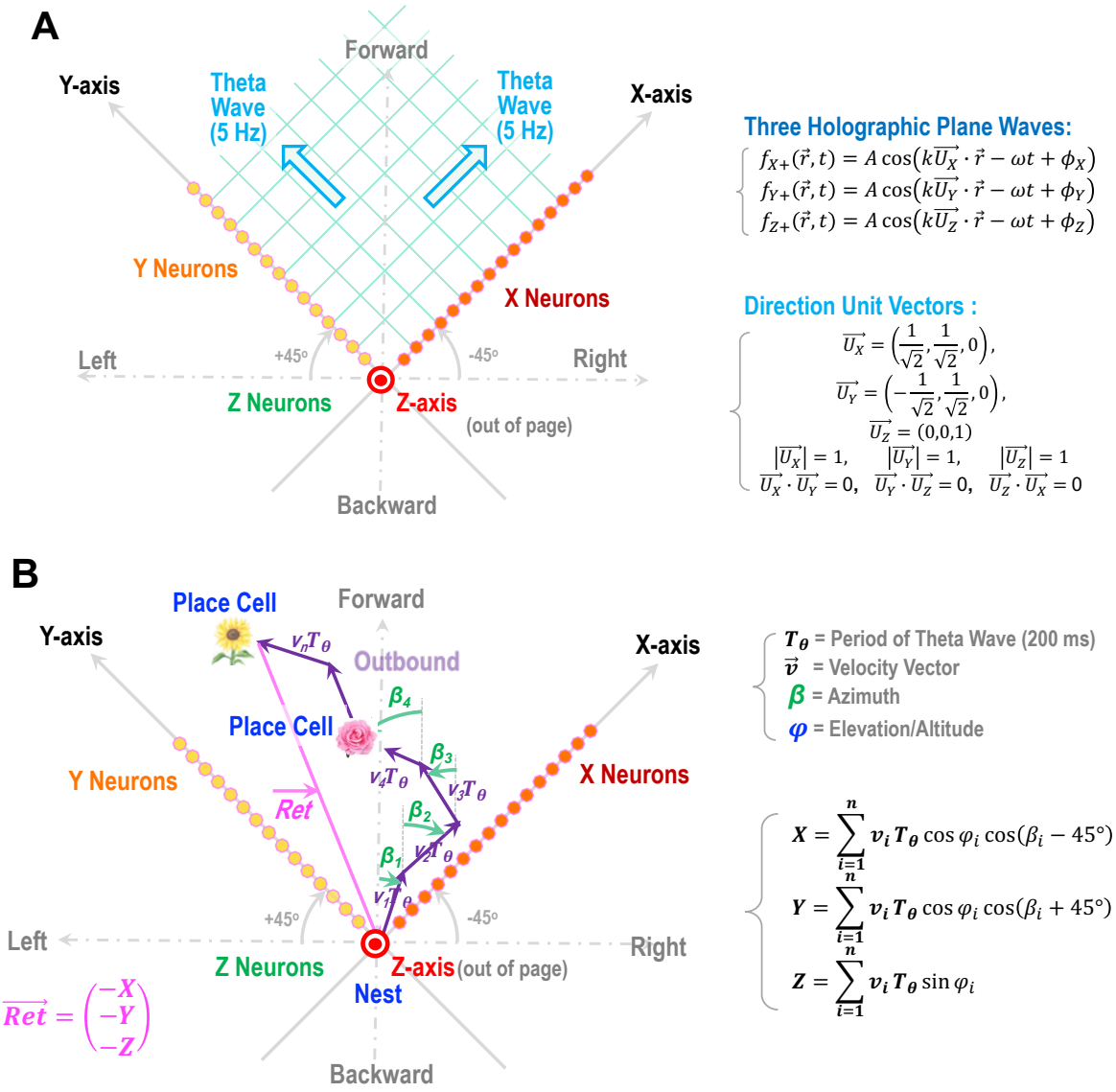

Figure 16. A possible navigation principle of birds (and perhaps insects). Insects might have a similar mechanism**. (A)** shows the three theta brainwaves, traveling to +/ 45° directions. **(B)** illustrates the principle of recording multiple landmarks by the place cells.

We will devote the entire **Part IV** to this navigation system. Here we briefly highlight a possible 3D Cartesian coordinate system, shown in **Figure 17**.

An essential point is that the observed grid cells exhibit a hexagonal pattern (Moser et al. 2008).. To derive the hexagonal geometry, let us introduce the specific Cartesian coordinate with hexagonally tilted three axes (X, Y, Z), which are still orthogonal to each other, as shown in **Figure 17**. Please consider this figure as the projected images of the 3D onto a 2D horizontal flat page, looking downward from the above. This is still a genuine 3D Cartesian coordinate frame, but it can generate an intriguing hexagonal pattern on the flat plane, which shows up by imposing the condition to form a horizontal flat plane, X+Y+Z = 0 (with the constraint of integers for all X, Y, and Z.) Under this restriction, the presented 2D coordinate system on a flat plane in **Figure 17** is called the Hexagonal Symmetrical Coordinate frame (Her 1992; Her 1995).

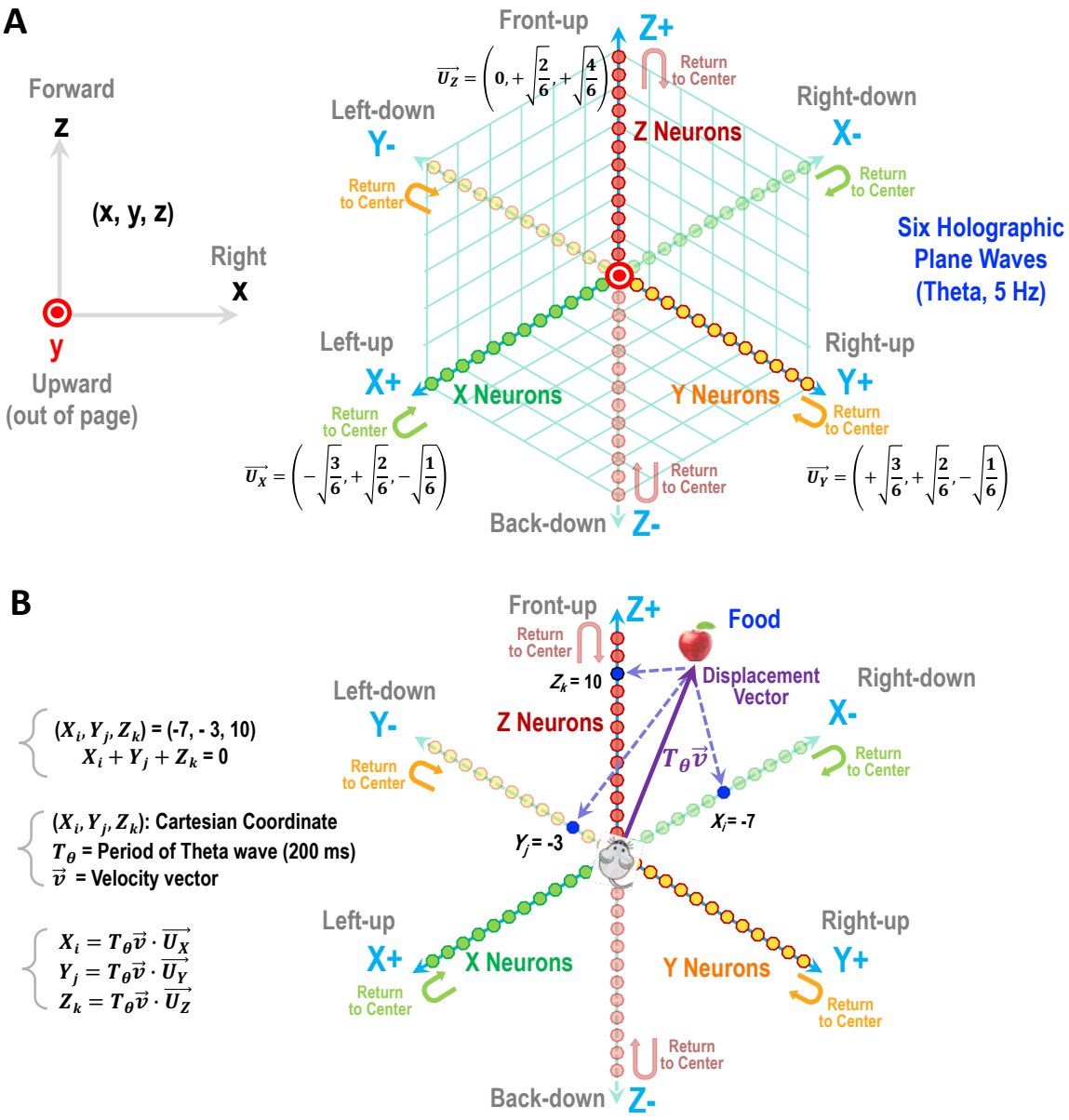

Figure 17. The tilted 3D Cartesian coordinate system of the navigation system. **(A)** shows six traveling waves. the unit vectors to the six directions are expressed by the regular 3D Cartesian coordinates, (x, y, z), on the left side of the figure. **(B)** shows an example of a landmark (= an apple) at Position (X_i, Y_j, Z_k) = (-7, -3, 10). The three assigned neurons (X_i = -7, Y_j = -3, Z_k =10) fire by coincidence when a rat arrives at that location of the apple. Therefore, these neurons are the place cells. The displacement vector expressed by the polar coordinate system is given here too.

Figure 17-B shows an example of a landmark (= an apple) at Cartesian Position (X_i, Y_j, Z_k) = (-7, -3, 10). The assigned three neurons (X_i = -7, Y_j = -3, Z_k =10) fire by coincidence, when a rat arrives at that location of the apple. Therefore, these neurons are the place cells in 3D. The displacement vector expressed by the polar coordinate system is given here too for convenience.

A more detailed complete treatment of the 3D navigation system will be given in **Part IV**.

7 HAL Acting as an *Engram*

7.1 Evolution from Spike Rate to Spike Timing

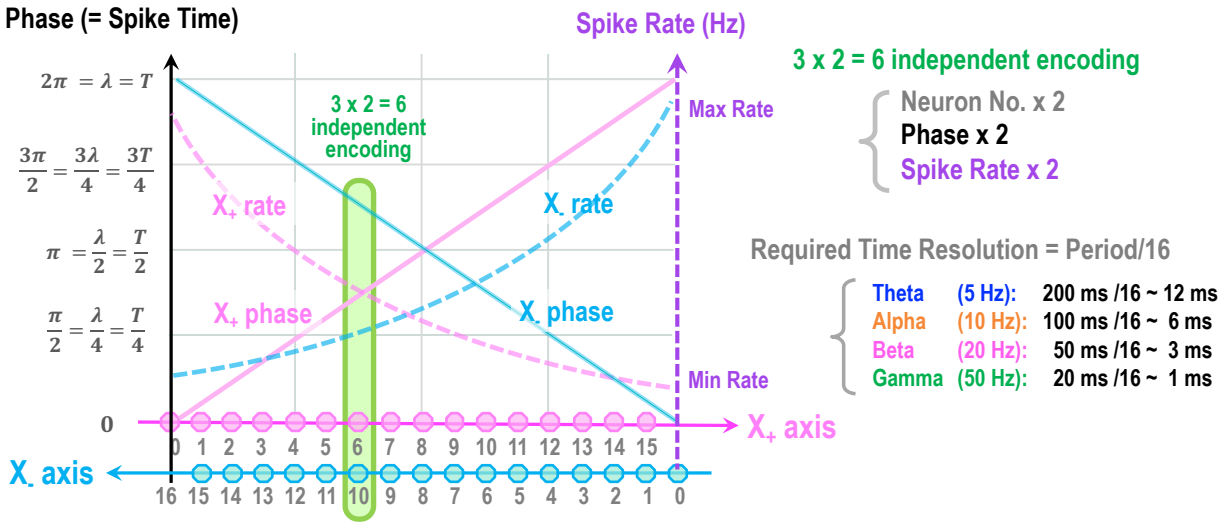

Figure 18. 3 x 2 = 6 independent coding schemes are involved in registering one specific location. At a given location of $X_+ = 6$, for example, $X_- = 10$ will fire together with specific spike timing and spike rates. This six-fold redundancy dramatically enhances the Signal-to-Noise ratio.

One may wonder whether such a holographic expression could have been an inevitable outcome of selective pressures in brain evolution. As we have discussed, the primary purpose of the brain is to enable safe and reliable navigation within allocentric 3D space to locations of food and back to the animal's nest. However, animals can only sense the environment in the egocentric frame, resulting in a non-trivial challenge of overcoming this fundamental mismatch between the allocentric and egocentric coordinate systems. Indeed, the ancestor of insects and other arthropods could well be the first organisms to have overcome this hurdle, as we have discussed already in **Section 1**. However, their navigation may rely on simple spike rates, which makes keeping track of multiple landmarks very difficult. It is also presumably impossible to memorize these multiple locations for revisits in the future. Therefore, it seems inevitable for animals more advanced than insects to have resorted to spike timings, rather than spike rates, for navigation processes as the next evolutionary step. We will extensively discuss this concept in **Part IV** with emphasis on the case of rodent hippocampal networks.

Nevertheless, evolution is not a revolution; the transition from spike rates to spike timings for space encoding must have been rather gradual; rate coding and time coding may even still co-exist today. **Figure 18** shows the redundant expression of space (only in 1D) by three independent variables: physical location in X, spike rate, and spike timing of the neuron. Furthermore, in our default definition of **HAL**, we consider two opposite directions of brainwaves along each axis. Therefore, a total of 3 (methods) x 2 (directions) = 6-fold redundant encodings could co-exist cooperatively. As shown in **Figure 18**, spike rate is likely to be to the highest at the center of the coordinate system (and in the forward direction), and it would gradually decay exponentially. At the given location of $X_+ = 6$, for example, $X_- = 10$ will fire together with the specific spike timings and spike rates shown in **Figure 18**. Such a sixfold redundancy could dramatically improve the signal-to-noise ratio for the reliable registration of locations.

7.2 Several Mechanisms to Reserve High Spatial Resolution

Let us next consider the expected accuracy of localization (i.e., the spatial resolution) by spike timing based on the brainwave phase. Generally speaking, around 10% temporal resolution of the period is feasible by assigning the specific phase. That is why 16 segments of linear neurons are assumed for the **HAL** in **Figure 11**. In the case of there being 16 segments (i.e., linear neurons on each axis) per period, the required resolution of spike timing (as given in **Figure 18**) is:

- Theta wave (5 Hz) → 200 ms / 16 ~ 12 ms
- Alpha wave (10 Hz) → 100 ms / 16 ~ 7 ms
- Beta wave (20 Hz) → 50 ms / 16 ~ 3 ms
- Gamma wave (50 Hz) → 20 ms / 16 ~ 1 ms

Past studies of spike-timing-dependent plasticity (STDP) show that, in the concept of Hebbian plasticity, the coincidence time window for long-term potentiation (LTP) is the order of milliseconds (Dan & Poo, 2004; Markram, Gerstner, & Sjöström, 2011). These findings are in support of our assumption of there being 16 segments per axis (i.e., per brainwave period). The case of gamma waves (~1 ms resolution) will be discussed later in **Part V** as a part of bottom-up signal processing. Most notably, Gray and Singer reported the gamma phase correlation to spike timing in the orientation column of the cat visual cortex with (0.4 ± 1.9)-millisecond accuracy in 1989 (Gray & Singer, 1989). Therefore, our assumption of ~1 ms resolution appears to be rational, even for high-frequency gamma waves (Fries, Nikolić, & Singer, 2007; Vinck, Womelsdorf, & Fries, 2013).

A new question naturally arises: why is our visual acuity far superior to 1/16 of the field of view? Our experience of visual acuity seems better than 1/1,000 in the field of view. In this regard, nature seems to have provided a unique solution to overcome this apparently poor spatial resolution. That is to utilize the Discrete Fourier Transformation (DFT). We will discuss it extensively in **Part IV** to explain the observed discrete patterns of grid cells.

Another possible solution comes from the direct linkage between top-down **HAL** (by theta/alpha/ beta waves) and bottom-up **HAL** (by gamma waves). Let's consider the linkage of a Theta (5 Hz) **HAL** and a Gamma **HAL** (50 Hz). The gamma waves, which are higher in frequency by a factor of ten, effectively work as a 10x magnifier for local regions of interest (ROI). Such a case is also considered in **Part IV**. The unification of top-down (by theta/alpha/ beta waves) and bottom-up (by gamma waves) processes will be discussed in **Part V**.

Lastly, saccadic eye movements can enhance visual acuity, combined with the log-polar coordinate system of the primary visual cortex to the ventral pathway. Wherever we need to see details, we re-allocate the fovea center to that direction by overt attention. Thanks to a dramatic magnification at the fovea center, the focused image can be viewed with superior resolution. Furthermore, constant micro-saccades can sample fine details as a function of time. We will discuss these effects in **Part IV**.

In summary, the above three mechanisms (DFT, the bottom-up gamma waves, saccades) are possibly working together to improve the visual acuity from 1/16 up to 1/1000, at least at the fovea center.

7.3 HAL as an Engram – Principle of Memory Mapping and Transfer

The critical feature of **HAL** is its function as an *engram* (Schacter, Eich, & Tulving 1978; Josselyn 2010; Josselyn & Tonegawa 2020; Eichenbaum 2016). As a universal memory unit, it should satisfy the standard criteria of a memory. The basic operations include Write, Erase, Read, Transfer, and Compare, much like a computer memory unit. Clearly, "Write" is achieved by long-term potentiation

(LTP) of STDP, whereas “Erase” is conducted the long-term depression (LTD). Meanwhile, “Read” is performed by specific brainwaves which scan the memory units.

A data “Transfer” from one **HAL** to another is carried out by the direct linkage of the two **HAL**s with the external 128 x 128 x 2 synapses in between, followed by the vibration of the **HAL**s with a shared brainwave. Thanks to the required precise coincidence (i.e., phase coherence), two distant **HAL**s can be faithfully linked, regardless of how they are separated in a broad cortical region. This is a remarkable feature that allows brain-wide communication, similar to communication via Wi-Fi or cell-phone networks today. Please note that such direct memory transfer can be conducted by arbitrary frequency all the way up to the high-frequency gamma waves (~100 Hz) or even higher frequency of sharp-wave ripples (SWR) as high as ~200 Hz. This could be a mechanism of the direct memory transfer from the Hippocampus CA1 to the Prefrontal Cortex for forming episodic memories. We will elaborate on this related to the navigation maps in **Part IV**. Furthermore, the origin of language and intelligence builds fundamentally on such broader cortical networks of numerous **HAL**s shared by multiple frequency bands, which will be discussed in **Part VI**.

Another remarkable feature is that **HAL** is a static synaptic memory, thus completely independent of frequency and phase by itself. Therefore, any frequency of brainwaves can read out with any desirable phase assignment. Taking advantage of the phase shift, we already demonstrated the remapping between the internal representation (perception) of allocentric 3D space and the egocentric sensory stimulation (**Section 3.3**); we can shift the location of a landmark in any 3D direction in up/down, left/right, forward/backward direction by a simple phase shift via the PN network. Also, the size of a landmark can be scaled up/down by assigning a higher/lower frequency brainwave.

Lastly, HAL is acting for all kinds of explicit memory, including

1) Episodic Memory
2) Semantic Memory
3) Working Memory
4) Short term / Long term Memory

Details of these memory formation will be given **in Part IV**.

In conclusion, remarkably, **HAL** appears to satisfy all required functions of a universal memory unit, an *engram*.

8 Grand Unification of Mind and Brain by HAL

8.1 The Universality of HAL for Five Senses

	Wave	Freq. (Hz)	Purpose	Dim.	Frame	Assignment of Eight Axes 1/2	3/4	5/6	7/8
Navigation									
	Theta	5	Space-time	4D	Allocentric	X	Y	Z	Time
	Beta	20	Direction Vector	3D	Allocentric	Azimuth/Yaw	Altitude/Pitch	Roll	Speed, Length
Vision									
	Alpha	8-12	3D Location	3D	Body-centric	Azimuth/Yaw	Altitude/Pitch	Depth	
	Alpha	8-12	2D Shape	2D	Object-centric	Eccentricity	Roll	(Scale)	(Rotation)
	Gamma	50-80	Local Shape	3D	(Bottom-up)	Local Orientation	Curvature	Kink	
	Gamma	40	Color (HSL)	3D	(Bottom-up)	Green-Red	Blue-Yellow	Lightness	
Sound									
	Alpha	8-12	3D Location	3D	Body-centric	Azimuth/Yaw	Altitude/Pitch	Depth	
	Alpha	8-12	Word	2D	Word-centric	Frequency	Modulation	Intensity	
	Gamma	70-150	Short Sound	2D	(Bottom-up)	Frequency	Modulation	Intensity	
Touch									
	Mu	8-13	3D Location	3D	Body-centric	Azimuth/Yaw	Altitude/Pitch	Depth	
	Gamma	30-90	Tactile	7D	Tactile	Pain A,B	Pressure A,B	Touch A,B	Touch C,D
Smell									
	Gamma	60	Olfactory	8D	Olfactory	Smell A,B	Smell C,D	Smell E,F	Smell, G,H
Taste									
	Delta	3	Taste	5D	Taste	Salty, Sweet	Sour, Bitter	Umami	

Table 3. A complete list of multiple brainwaves and their functions (already introduced in **Part I: Table 3.)** These brainwaves are responsible for the holographic representation of a certain space: either real 3D space, or extra sensory dimensions such as touch, smell, and taste. Generally speaking, the top-down predictions are carried by low-frequency brainwaves (Theta, Alpha, Beta), whereas higher-frequency gamma bands carry bottom-up sensory signals. Details will be given in **Part V**.

Before ending this **Part II: Neural Holographic Tomography (NHT) and Holographic Ring Attractor Lattice (HAL)**, let us list all possible **HAL**s in human brain in **Table 3**. This table includes the **HAL**s generated by high-frequency gamma waves for the five senses.

So far **in Part II**, we have considered 3D navigation and visual perception by the three low-frequency brainwaves: Theta (~5 Hz), Alpha (~10 Hz), and Beta (~20 Hz).

1) The beta wave (~20 Hz) is to track 3D head direction in the polar coordinate system (**Section 5.2**).
2) The alpha wave (~10 Hz) is for 3D vision via the visual pathways (**Section 5.3**).
3) The theta wave (~5 Hz) is for 3D/4D navigation via the Hippocampal network (**Section 6.3**).

In **Part III** and **IV,** we will further explore how these brainwaves – especially alpha and theta waves – holographically express 3D space and shape by their phases.

In addition to the visual perception of 3D space, we can localize sound sources in 3D space as well. Furthermore, tactile sensation can also be vividly localized in 3D. Thanks to the universality of **HAL**, three-fold agreement of 3D locations by three independent sensations could occur naturally in the frequency-time domain. This will be discussed in **Part V**.

High-frequency gamma brainwaves are essential for bottom-up sensory signal processing for all five senses, including:

1) Local shape (line orientation, kinks, curvatures)
2) Local colors (hue, saturation, brightness)
3) Pitch and amplitude modulation of instantaneous sound
4) Tactile sensation on the skin
5) Smell and taste

The detailed mechanisms of these bottom-up processes for all five senses will be presented in **Part V**.

8.2 Summary – Holographic Ring Attractor Lattice (HAL)

In this **Part II**, we defined **Holographic Ring Attractor Lattice (HAL)** as a possible candidate for the *engram*. It is a natural extension of insects' ring attractors and capable of encoding 3D space (or 4D space-time) and 3D shape in the form of compact 2D metric of synaptic connections, which is 100% consistent with Hebbian plasticity. It elegantly explains the observed place cells, time cells, grid cells, head direction cells, and speed cells altogether by the unifying principle.

Utilizing the **HAL**, we have successfully covered various aspects of the **Grand Unification of Mind and Brain** as follows.

1) Unification of 3D visual perception (by alpha) and 3D navigation (by theta): **Sections 2** and **3**
2) Unification of covert attention and overt attention: **Section 3.3**
3) Unification of different coordinate systems: Cartesian vs. Polar, Linear vs. Log: **Section 4**
4) Unification of navigation: path integration (beta) and place/grid cells (theta): **Sections 5** and **6**
5) Unification of signal carriers: spike rates and spike timing (by brainwave phases): **Section 7.1**
6) Unification of various explicit memories: **7.3**

Finally, the essential groundworks of **MePMoS**, **NHT**, and **HAL** have been completed. By applying these, we shall now continue the remaining story of the "**Grand Unified Theory of Mind and Brain"** in the following order.

Part III. Holographic Visual Perception of 3D Space and Shape
Part IV. Navigation and Episodic Memory by the Hippocampal Network
Part V. Grand Unification of Five Senses and Memories
Part VI. The Origin of Language, Consciousness, and Intelligence

Through these four parts, we will explore all types of cognitive processes listed below, step by step:

1) Extraction of semantic information (such as a human face) via the ventral visual pathway: **Part III**
2) Visual perception of allocentric 3D space via the dorsal visual pathway: **Part III**
3) Navigation and Memorization of external 3D space by the Hippocampal network: **Part IV**
4) Conversion of episodic memories to semantic memories: **Section IV**
5) Unified 3D localization by vision, hearing, and touch (by alpha): **Part V**
6) Unification of all five senses: vision, hearing, touch, smell, taste (by gamma): **Part V**
7) The origin of language and logical thought: **Section VI**
8) The origin of consciousness, intelligence, and creativity: **Section VI**

Acknowledgments

The author thanks Aaron Blaisdell for extensive discussion throughout the development of the concepts of **NHT** and **HAL** for the last four years. Many new ideas in this **Part II** are the outcome of our weekly conversation. I also thank him for carefully reading and editing this paper.

Syed Hydari contributed to developing new concepts in the early stage. Discussion with Zahra Aghajan for the last three years was useful to fine-tune the theory in **Part II**. I thank Ziyan Peng for her careful editing of the initial manuscript.

This work was in part supported by the Dean's office of life science, Dean's office of physical science, Chair's office of the department of physics and astronomy, and the Instructional Improvement grant by the Center for the Advancement of Teaching, all at the University of California, Los Angeles.

References

Abdollahi, Rouhollah O., Hauke Kolster, Matthew F. Glasser, Emma C. Robinson, Timothy S. Coalson, Donna Dierker, Mark Jenkinson, David C. Van Essen, and Guy A. Orban. 2014. "Correspondences between Retinotopic Areas and Myelin Maps in Human Visual Cortex." *NeuroImage* 99:509–24. doi: 10.1016/j.neuroimage.2014.06.042.

Altun, Herndon, Wolkow, Crocker, Lints, and Hall. 2021. "WormAtlas: Http://Www.Wormatlas.Org."

Arendt, Detlev, Maria Antonietta Tosches, and Heather Marlow. 2016. "From Nerve Net to Nerve Ring, Nerve Cord and Brain — Evolution of the Nervous System." *Nature Reviews Neuroscience* 17(1):61–72. doi: 10.1038/nrn.2015.15.

Arisaka, Katsushi. 2022. "Grand Unified Theory of Mind and Brain - Part I: Space-Time Approach to Dynamic Connectomes of C. Elegans and Human Brains by MePMoS."

Benson, Noah C., Omar H. Butt, David H. Brainard, and Geoffrey K. Aguirre. 2014. "Correction of Distortion in Flattened Representations of the Cortical Surface Allows Prediction of V1-V3 Functional Organization from Anatomy" edited by W. Einhäuser. *PLoS Computational Biology* 10(3):e1003538. doi: 10.1371/journal.pcbi.1003538.

Bridge, Holly, David A. Leopold, and James A. Bourne. 2016. "Adaptive Pulvinar Circuitry Supports Visual Cognition." *Trends in Cognitive Sciences* 20(2):146–57. doi: 10.1016/j.tics.2015.10.003.

Buzsáki, György. 2006. *Rhythms of the Brain*. Oxford University Press.

Buzsáki, György. 2015. "Hippocampal Sharp Wave-Ripple: A Cognitive Biomarker for Episodic Memory and Planning: HIPPOCAMPAL SHARP WAVE-RIPPLE." *Hippocampus* 25(10):1073–1188. doi: 10.1002/hipo.22488.

Buzsáki, György. 2018. "Space and Time: The Hippocampus as a Sequence Generator: Trends in Cognitive Sciences." Retrieved March 13, 2020 (https://www.cell.com/trends/cognitive-sciences/fulltext/S1364-6613(18)30166-9).

Caves, Eleanor M., Nicholas C. Brandley, and Sönke Johnsen. 2018. "Visual Acuity and the Evolution of Signals." *Trends in Ecology & Evolution* 33(5):358–72. doi: 10.1016/j.tree.2018.03.001.

Coulon, Philippe, and Carole E. Landisman. 2017. "The Potential Role of Gap Junctional Plasticity in the Regulation of State." *Neuron* 93(6):1275–95. doi: 10.1016/j.neuron.2017.02.041.

Dan, Yang, and Mu-ming Poo. 2004. “Spike Timing-Dependent Plasticity of Neural Circuits.” *Neuron* 44(1):23–30. doi: 10.1016/j.neuron.2004.09.007.

DiCarlo, James J., Davide Zoccolan, and Nicole C. Rust. 2012. “How Does the Brain Solve Visual Object Recognition?” *Neuron* 73(3):415–34. doi: 10.1016/j.neuron.2012.01.010.

Eichenbaum, Howard. 2016. “Still Searching for the Engram.” *Learning & Behavior* 44(3):209–22. doi: 10.3758/s13420-016-0218-1.

Etienne, Ariane S., and Kathryn J. Jeffery. 2004. “Path Integration in Mammals.” *Hippocampus* 14(2):180–92. doi: 10.1002/hipo.10173.

Felleman, Daniel J., and David C. Van Essen. 1991. “Distributed Hierarchical Processing in the Primate Cerebral Cortex.” *Cereb Cortex* 1–47.

Fisher, Yvette E., Jenny Lu, Isabel D’Alessandro, and Rachel I. Wilson. 2019. “Sensorimotor Experience Remaps Visual Input to a Heading-Direction Network.” *Nature* 576(7785):121–25. doi: 10.1038/s41586-019-1772-4.

Fries, Pascal, Danko Nikolić, and Wolf Singer. 2007. “The Gamma Cycle.” *Trends in Neurosciences* 30(7):309–16. doi: 10.1016/j.tins.2007.05.005.

Gabor, Dennis. 1948. “A New Microscopic Principle.” *Nature* 161(4098):777–78. doi: 10.1038/161777a0.

Garrett, M. E., I. Nauhaus, J. H. Marshel, and E. M. Callaway. 2014. “Topography and Areal Organization of Mouse Visual Cortex.” *Journal of Neuroscience* 34(37):12587–600. doi: 10.1523/JNEUROSCI.1124-14.2014.

Gilbert, Charles D., and Wu Li. 2013. “Top-down Influences on Visual Processing.” *Nature Reviews Neuroscience* 14(5):350–63. doi: 10.1038/nrn3476.

Gray, C. M., and W. Singer. 1989. “Stimulus-Specific Neuronal Oscillations in Orientation Columns of Cat Visual Cortex.” *Proceedings of the National Academy of Sciences* 86(5):1698–1702. doi: 10.1073/pnas.86.5.1698.

Her, I. 1992. “A Symmetrical Coordinate Frame on the Hexagonal Grid for Computer Graphics and Vision.” Pp. 187–90 in. American Society of Mechanical Engineers Digital Collection.

Her, I. 1995. “Geometric Transformations on the Hexagonal Grid.” *IEEE Transactions on Image Processing* 4(9):1213–22. doi: 10.1109/83.413166.

Honkanen, Anna, Andrea Adden, Josiane da Silva Freitas, and Stanley Heinze. 2019. “The Insect Central Complex and the Neural Basis of Navigational Strategies.” *The Journal of Experimental Biology* 222(Suppl 1):jeb188854. doi: 10.1242/jeb.188854.

Horton, Jonathan C., and William F. Hoyt. 1991. “The Representation of the Visual Field in Human Striate Cortex: A Revision of the Classic Holmes Map.” *Archives of Ophthalmology* 109(6):816–24. doi: 10.1001/archopht.1991.01080060080030.

Jones, Matthew W., and Matthew A. Wilson. 2005. “Phase Precession of Medial Prefrontal Cortical Activity Relative to the Hippocampal Theta Rhythm.” *Hippocampus* 15(7):867–73. doi: 10.1002/hipo.20119.

Josselyn, Sheena A. 2010. “Continuing the Search for the Engram: Examining the Mechanism of Fear Memories.” *Journal of Psychiatry & Neuroscience : JPN* 35(4):221–28. doi: 10.1503/jpn.100015.

Josselyn, Sheena A., and Susumu Tonegawa. 2020. “Memory Engrams: Recalling the Past and Imagining the Future.” *Science* 367(6473):eaaw4325. doi: 10.1126/science.aaw4325.

Koizumi, Osamu. 2007. “Nerve Ring of the Hypostome in Hydra: Is It an Origin of the Central Nervous System of Bilaterian Animals?” *Brain, Behavior and Evolution* 69(2):151–59. doi: 10.1159/000095204.

Koizumi, Osamu, Shun Hamada, Sumiko Minobe, Kayoko Hamaguchi-Hamada, Mami Kurumata-Shigeto, Masaru Nakamura, and Hiroshi Namikawa. 2015. “The Nerve Ring in Cnidarians: Its Presence and Structure in Hydrozoan Medusae.” *Zoology* 118(2):79–88. doi: 10.1016/j.zool.2014.10.001.

Kropff, Emilio, James E. Carmichael, May-Britt Moser, and Edvard I. Moser. 2015. “Speed Cells in the Medial Entorhinal Cortex.” *Nature* 523(7561):419–24. doi: 10.1038/nature14622.

Kruger, N., P. Janssen, S. Kalkan, M. Lappe, A. Leonardis, J. Piater, A. J. Rodriguez-Sanchez, and L. Wiskott. 2013. “Deep Hierarchies in the Primate Visual Cortex: What Can We Learn for Computer Vision?” *IEEE Transactions on Pattern Analysis and Machine Intelligence* 35(8):1847–71. doi: 10.1109/TPAMI.2012.272.

Lisman, John, György Buzsáki, Howard Eichenbaum, Lynn Nadel, Charan Ranganath, and A. David Redish. 2017. “Viewpoints: How the Hippocampus Contributes to Memory, Navigation and Cognition.” *Nature Neuroscience* 20(11):1434–47. doi: 10.1038/nn.4661.

Llinas, Rodolfo R. 2014. “Intrinsic Electrical Properties of Mammalian Neurons and CNS Function: A Historical Perspective.” *Frontiers in Cellular Neuroscience* 8. doi: 10.3389/fncel.2014.00320.

Lozano-Soldevilla, Diego, and Rufin VanRullen. 2019. “The Hidden Spatial Dimension of Alpha: 10-Hz Perceptual Echoes Propagate as Periodic Traveling Waves in the Human Brain.” *Cell Reports* 26(2):374-380.e4. doi: 10.1016/j.celrep.2018.12.058.

Lyu, Cheng, L. F. Abbott, and Gaby Maimon. 2020. *A Neuronal Circuit for Vector Computation Builds an Allocentric Traveling-Direction Signal in the* Drosophila *Fan-Shaped Body*. *preprint*. Neuroscience. doi: 10.1101/2020.12.22.423967.

Markram, Henry, Wulfram Gerstner, and Per Sjöström. 2011. “A History of Spike-Timing-Dependent Plasticity.” *Frontiers in Synaptic Neuroscience* 3:4. doi: 10.3389/fnsyn.2011.00004.

Medina, Loreta. 2010. “Do Birds and Reptiles Possess Homologues of Mammalian Visual, Somatosensory, and Motor Cortices?” *Evolution of Nervous Systems* 2:163–94. doi: 10.1016/B0-12-370878-8/00132-4.

Meer, Matthijs A. A. van der, and A. David Redish. 2011. “Theta Phase Precession in Rat Ventral Striatum Links Place and Reward Information.” *Journal of Neuroscience* 31(8):2843–54. doi: 10.1523/JNEUROSCI.4869-10.2011.

Moser, Edvard I., Emilio Kropff, and May-Britt Moser. 2008. “Place Cells, Grid Cells, and the Brain’s Spatial Representation System.” *Annual Review of Neuroscience* 31(1):69–89. doi: 10.1146/annurev.neuro.31.061307.090723.

Murata, Akira, Wen Wen, and Hajime Asama. 2016. “The Body and Objects Represented in the Ventral Stream of the Parieto-Premotor Network.” *Neuroscience Research* 104:4–15. doi: 10.1016/j.neures.2015.10.010.

Nériec, Nathalie, and Claude Desplan. 2016. “From the Eye to the Brain.” Pp. 247–71 in *Current Topics in Developmental Biology*. Vol. 116. Elsevier.

O’Keefe, John. 1976. “Place Units in the Hippocampus of the Freely Moving Rat.” *Experimental Neurology* 51(1):78–109. doi: 10.1016/0014-4886(76)90055-8.

Otsuna, Hideo, Kazunori Shinomiya, and Kei Ito. 2014. “Parallel Neural Pathways in Higher Visual Centers of the Drosophila Brain That Mediate Wavelength-Specific Behavior.” *Frontiers in Neural Circuits* 8. doi: 10.3389/fncir.2014.00008.

Pegel, Uta, Keram Pfeiffer, Frederick Zittrell, Christine Scholtyssek, and Uwe Homberg. 2019. “Two Compasses in the Central Complex of the Locust Brain.” *The Journal of Neuroscience* 39(16):3070–80. doi: 10.1523/JNEUROSCI.0940-18.2019.

Petersen, Carl C. H. 2007. “The Functional Organization of the Barrel Cortex.” *Neuron* 56(2):339–55. doi: 10.1016/j.neuron.2007.09.017.

Sato, Makoto, Takumi Suzuki, and Yasuhiro Nakai. 2013. “Waves of Differentiation in the Fly Visual System.” *Developmental Biology* 380(1):1–11. doi: 10.1016/j.ydbio.2013.04.007.

Schacter, Daniel L., James Eric Eich, and Endel Tulving. 1978. “Richard Semon’s Theory of Memory.” *Journal of Verbal Learning and Verbal Behavior* 17(6):721–43. doi: 10.1016/S0022-5371(78)90443-7.

Schwenk, Kurt. 1994. “Why Snakes Have Forked Tongues.” 263:5.

Skaggs, William E., Bruce L. McNaughton, Matthew A. Wilson, and Carol A. Barnes. 1996. “Theta Phase Precession in Hippocampal Neuronal Populations and the Compression of Temporal Sequences.” *Hippocampus* 6(2):149–72. doi: https://doi.org/10.1002/(SICI)1098-1063(1996)6:2<149::AID-HIPO6>3.0.CO;2-K.

Soares, Sandra C., Rafael S. Maior, Lynne A. Isbell, Carlos Tomaz, and Hisao Nishijo. 2017. “Fast Detector/First Responder: Interactions between the Superior Colliculus-Pulvinar Pathway and Stimuli Relevant to Primates.” *Frontiers in Neuroscience* 11. doi: 10.3389/fnins.2017.00067.

Stone, Thomas, Barbara Webb, Andrea Adden, Nicolai Ben Weddig, Anna Honkanen, Rachel Templin, William Wcislo, Luca Scimeca, Eric Warrant, and Stanley Heinze. 2017. “An Anatomically Constrained Model for Path Integration in the Bee Brain.” *Current Biology* 27(20):3069-3085.e11. doi: 10.1016/j.cub.2017.08.052.

Taube, Jeffrey S. 2007. “The Head Direction Signal: Origins and Sensory-Motor Integration.” *Annual Review of Neuroscience* 30(1):181–207. doi: 10.1146/annurev.neuro.29.051605.112854.

Vinck, Martin, Thilo Womelsdorf, and Pascal Fries. 2013. “Gamma-Band Synchronization and Information Transmission.” Pp. 449–70 in *Principles of Neural Coding*. CRC Press.

Ward, S. 1973. “Chemotaxis by the Nematode Caenorhabditis Elegans: Identification of Attractants and Analysis of the Response by Use of Mutants.” *Proceedings of the National Academy of Sciences of the United States of America* 70(3):817–21. doi: 10.1073/pnas.70.3.817.

Wiestler, Tobias, David J. McGonigle, and Jörn Diedrichsen. 2011. “Integration of Sensory and Motor Representations of Single Fingers in the Human Cerebellum.” *Journal of Neurophysiology* 105(6):3042–53. doi: 10.1152/jn.00106.2011.

Willemink, Martin J., and Peter B. Noël. 2019. “The Evolution of Image Reconstruction for CT—from Filtered Back Projection to Artificial Intelligence.” *European Radiology* 29(5):2185–95. doi: 10.1007/s00330-018-5810-7.